CYCLIC LATERAL LOADING OF PILES; ANALYSIS OF CENTRIFUGE TESTS

Ronald F. Scott

Report Through May 31, 1979
Research Program

for

American Petroleum Institute
OSAPR Project 13

June 4, 1979

Soil Mechanics Laboratory
Division of Engineering and Applied Science
California Institute of Technology
Pasadena, California 91125

ERRATA

Page	Line	Wrong	Right
2	10	--other pile studies--	--another pile study--
8	Footnote	--polynomial functions only use--	--polynomial functions in standard routines only use
19	15	--ℓ, m, and u--	--ℓ, m, and n--
20	Eqn. (4.2.1.1)	--u* = -0.444--	--u* = -0.444[1]--- and add footnote "[1]This result comes from an equation for u* similar to those of equation (4.2.2)."
22	17	--upwards to--	--up towards--
23	12,21	--(A.1.12)--	--(A:1.14)--
24	8	--(A.1.12)--	--(A.1.14)--
26	Fig. 3	--split fit--	--spline fit--
32	Fig. 3	--split fit--	--spline fit--
34,35	Fig. 4		It is not mentioned in the text, that, by mistake, the moments were made equal to zero at 325 inch depth in this case. Since the results, Figure 4(b) were so poor, the case was not run again with corrected input data.
26,49	Fig. 12		Add sentence to caption: "The curves B and D with exponents 1.5 and 1.0 (implied) respectively were drawn by hand through the data points."
27,50	Fig. 13	--Equation (A.1.12)--	--Equation (A.1.14)--
27,50	Fig. 13		Add sentence to caption: "The curves are drawn for equal increments in friction angle from 30^{o} (lowest curve) to 50^{o} (highest curve)."
27,51	Fig. 14	--Equation (A.1.12)--	--Equation (A.1.14)--
56	15	--be ignored.--	--be ignored, except for displacements just outside the elastic/-plastic transition.
56	last	(A.1.12)	(A.1.14)
57	first	--log F versus	--log F versus log u, when the full form of f in equation (A.1.13) is used in equation (A.1.14), tends--

1. Introduction

1.1 Summary of Previous Work

In two previous reports (6,7) results were given of a number of cyclic lateral load tests on model piles loaded in a centrifuge. The tests results were obtained in the form of loads and deflections at the top of the pile and readings from strain gauges distributed down the pile; the latter are interpreted in the form of moments. In contrast to field tests, the centrifuge pile experiments are carried out in an extremely uniform medium consisting, in the tests discussed, of dry and wet sand in two test series. The result of this soil uniformity is that moment readings can be represented by a smooth and continuous curve. Erratic data due to alternately dense and loose soil layers are avoided. In the second report (7) the fitting of curves to this data was discussed briefly with reference to the use of a fifth-order spline function. The advantage of the technique is that the curve passes through all the data points in contrast with least squares or linear regression fits. In the latter, general curves are obtained representative of the pile deflections in some way which pass near but not necessarily through the data points. Errors in the data are inherently accepted in this method.

In addition, the spline fit can be adapted to the boundary conditions at both ends of the pile so that these requirements can be met exactly by the functions selected. For example at the point of lateral load application to the pile top, the moment is zero. However, the derivative of the moment is the lateral load in the pile, and this value is known at the pile top during the experiment. Also, the second derivative is the soil reaction on the pile, and, in sand, this must be zero at the pile

top. The smoothness of the spline fit to the moment data is good enough to suggest the possibility of carrying out double integrations and double differentiations of the moment (with a multiplicative constant, EI) in order to get information on the pile deflections and pressure acting on the pile as a function of depth. Curves of deflection and pressure were presented in the second report, although no interpretation of the data at that stage of the investigation had been attempted.

No *a priori* assumptions regarding soil-pile interaction pressure either as a function of pile deflection or with depth are involved in the spline-fitting approach. In other pile studies (2) carried out on prototype piles in natural soil deposits, some scatter in strain-gauge (moment) data were inevitable and led to fitting difficulties. In consequence, a model for pile-soil behavior was adduced in that investigation, and the fitting method consisted of finding for that model those soil properties which gave smooth moment curves best representing the data observed. Such an approach does not inform the investigator of the real soil-pile behavior developed. For example, since, in all soils, a lateral load applied to the pile at ground surface will develop a moment curve which resembles a damped sine wave, it would be possible to use the well-known Winkler foundation solution for a laterally-loaded pile imbedded in a medium of constant spring property k, where the pile moment M is given by the equation

$$M = \frac{P}{\lambda} e^{-\lambda z} \sin \lambda z \qquad (1.1.1)$$

where $\lambda = \sqrt[4]{\frac{k}{4EI}}$, and z is distance down the pile measured from the point of load application. Superficially, this equation looks like the centrifuge

test results, and, by least squares fit, a value of λ could be found for which any one moment curve could be best fitted. However, the second derivative of equation (1) gives a finite value for the soil pressure at $z = 0$, and this would clearly not be representative of the sand behavior, dry or wet, at the top of the pile. In addition, of course, a different value of λ would be required to fit each moment curve produced by each lateral load. A general theory of soil-pile behavior would be difficult to extract from such a process.

It is the purpose of this report to take the centrifuge data analysis to a further stage to examine the interaction between pile and soil as a function of manipulation of the test results and the fitting techniques, with the fewest assumptions.

1.2 Problems With Fitting Technique

In the second report it is apparent that the spline functions give smooth curves fitting the moment data extremely well and to some extent confirming that the data are a reliable indication of the pile response in a uniform soil. When the spline functions are differentiated once, the resulting curve gives the distribution of shear force in the pile. One of the requirements made in the fitting process was that the shear force at the top of the pile should equal the known applied load. Consequently, a fair degree of confidence can be placed in the shear force versus depth curves since they are correct at the extreme vaue at the top of the pile.

Similarly when the moment curves are divided by the product EI and integrated once, the result is the slope of the pile as a function of

depth. A further integration of the slope gives the displacement at the pile top. Since the displacement was measured in the course of the test, the second integral curve can be checked at the extreme point again, that is, at ground surface. When this was done, it was found that the ground surface deflections obtained from the two integrations were very close to the deflections actually measured at different loads in the test. Consequently it seems likely that the deflection data as a function of depth obtained by two integrations are also reliable. It is of course well-known that integrations of even poor quality data can lead to reasonably reliable results. Differentiation is another matter, however.

Although there is control over the first differentiation of the moment curves, the identification of the pressure acting on the pile from the soil surrounding it depends on a second differentiation. It would be anticipated that this might give rise to problems, and, in fact, there has been discussion in the literature of the possible introduction of errors by such double differentiation (2,5). However in field tests on instrumented piles, there has been no control over the nature of the soil, which, in general, has been a relatively nonuniform or layered material. In consequence, the moment data recorded in field tests exhibits a fair degree of scatter and the application of spline fitting methods to such scattered points would not be expected to be reliable. In consequence either hand fitting or regression techniques of curve fitting must be applied to such field data. The greater uniformity of the centrifuge test soil and the smoothness of the original spline fitting technique give some hope that the second derivative of the present data may not be subjected to as great errors as in former field test fitting processes.

With the fifth-order spline the second derivative curves are of course smooth and continuous; the question is whether they can be believed to be numerically accurate for the purpose of further interpretation of the soil behavior. In Figure 1 are shown the pressure distribution curves for the first cycle of loading and unloading in the tests carried out on the pile in dry and wet sand, respectively. These curves represent the derived distribution of the interaction between the pile and the soil as a function of depth. Although they are referred to as pressure curves, some care must be taken in understanding the meaning of this phrase. As a portion of the pile below the surface deflects horizontally under the surface loading, the soil in front of the pile will be compressed and displaced, exerting some pressure in the process on the front surface of the pile. The soil along the side of the pile will be largely subjected to more or less simple shearing behavior and will interact with the pile through shearing stresses. On the rear surface of the pile, the pile is moving away from the soil and the lateral soil pressures developed during pile driving will be reduced as the pile retreats. The curves shown in Figure 1 represent the cumulative effect on the pile of all these mechanisms of behavior. Are they reasonable in appearance?

At the ground surface the pile is displaced laterally with a deflection which decreases rapidly with depth. It is expected that the soil interaction resistance increases with depth from zero at the surface because of the increasing confining pressure in the cohesionless soil of the test. The combination of increasing soil resistance and decreasing pile deflection with depth should cause the soil pressure to reach some maximum value below which it decreases. At some depth below the surface

the pile deflection is zero and consequently the pressure distribution should go through zero at this point. Below this the pile has a retrograde motion. Consequently in this region it is expected that the net soil pressure would be in the opposite direction. This is referred to here as negative pressure, compared to the positive pressure in the upper section of the pile.

It is apparent from Figure 1 that neither of the two derived pressure distributions for the pile response in the dry or the wet soil corresponds to this logical model. In both cases to a depth of something like 8 or 9 inches below ground surface it can be seen that small pressures, both negative and positive, occur. The pressures during the first loading phase only begin to increase consistently at depths below this level. An indication of negative pressure in the soil in the top eight inches therefore represents an error in the manipulation of the data. It might develop either as a consequence of cumulative errors in the strain gauge readouts and calibration, or in digitization and processing of the data. Alternatively, if small errors can be accepted in these aspects of the analysis the difference between the interpreted and the logical or correct distribution of pressures may be due to the spline fitting process. Since a check of the cumulative calibration and digitizing errors indicated that they were fairly small, it was decided to make the assumption that the moment data could be accepted, and that better distributions of the pressure acting on the pile could be derived by manipulating the spline function or by other methods of fitting the data. This is discussed subsequently.

1.3 Further Investigations

Several different approaches were taken to the fitting problem and are described in subsequent sections of this report. Initially attempts involved other forms of function. After devoting a small amount of time to this, it was decided that it was not a fruitful way to proceed in view of the good fits achieved with the spline function. Consequently attention was paid to manipulating the spline-fitting technique to give more rational results in the top section of the pile.

One of these involved omitting the top data point (moment) and utilizing only the moments at the five other locations as well as the top and bottom boundary conditions in the pile. This, as will be shown subsequently, gave rise to pressure distributions which were obviously incorrect and considerably worse than the ones which had been obtained before.

After careful study of the method by which the tests had been conducted in the centrifuge, it was concluded that the soil level was not necessarily accurately located with respect to the application of the load. In the tests, it was intended to have the filament applying the load act exactly at ground surface. This implies the identification of ground surface quite accurately for the following reason. The tests were conducted at 100g on a 1/100 scale model pile. All linear dimensions in the experiment, therefore, including deflections, were 1/100 of those of the prototype pile. Consequently, if the point of attachment of the lateral load to the pile top was in error with respect to the soil level by 1/100 of an inch, it means that the prototype pile was loaded at a point one inch different from that intended. With prototype loads of

30 or 40 Kips, the moment at the point interpreted to be ground surface could be different from zero by a substantial amount. It is difficult in the model to measure the attachment point initially to this level of accuracy, and during the cyclic loading tests, the soil level changes by an unknown amount. Accordingly it was decided to move the zero moment point on the pile up or down by small amounts in the analysis in order to examine the effect on the spline-fitting technique. The consequences are discussed in detail in the following sections.

2. Fitting Attempts

2.1 Various Functions

Fits to the moment data were attempted using polynomials of order eight to ten. Although these could reasonably fit the moment data obtained passing close to but not through the moment points, the functions deviate wildly from the known behavior of the pile below the level of the last moment point. They only fit the data in the range prescribed.* In this sense, from a theoretical point of view, they are the wrong functions to work with. When it became obvious that their fit was considerably worse than that of the spline functions and that the integrations and differentiations gave results poorer than even the initial attempt at spline fitting, this approach was abandoned.

Some time was spent in looking at different rational functions which might be logically employed to fit the shape of the moment curves. In general these were obtained from functions derived by assuming that the pile-soil interaction could be described by Winkler foundation-beam equations. Presumably if the soil response as a function of depth could

---

* Besides, polynomial functions only use the given points; they make no use of information supplied by derivatives of the moment at pile top and bottom.

be represented reasonably closely, this method might give quite good results and indeed can be taken to be one of the objectives of the investigation. However, the assumption of curves based on a particular behavior (for example that the soil resistance increases linearly with depth) automatically will give rise to that kind of behavior when the integrations and differentiations have been made, so the process does not clarify the mechanisms actually taking place. The advantage of the spline fits is that they require no *a priori* assumptions regarding the nature of moment distribution, pile deflection or soil resistance. Their disadvantage is that, by passing through all the measured data points, they make no allowance for scatter in the data, due to soil response or measurement error. Spline functions would not, for example, be suitable fits to the field moment data obtained in the Mustang Island pile tests (5).

2.2 Variations in Spline Fitting Method (1)

A first attempt was to examine a cubic rather than a fifth-order fit to the dry test first cycle data to see if the simpler function would make clearer the errors involved in the analysis. Figure 2a and b show the result of this application to the dry sand test in terms of moment and pressure distribution, respectively. From Figure 2a little difference is apparent in the curves of moment distribution from those in the previous report (7) for the fifth-order spline. However, with the cubic spline two differentiations of course give rise to a series of straight line segments between the levels at which the moments were measured. This can be seen in Figure 2b in which the kink in the pressure

distribution in the top few inches of the pile can again be seen, although it is not as strongly apparent as in Figure 1a. Although it might have been possible to fit another function to the pressure distribution or to obtain further information by manipulating that data, the clearly linear segments so obviously do not fit a logically smooth pressure variation that this approach was not used further.

For another attempt it was considered that the top moment data point might be in error and giving rise to a misleading effect on the pressure distribution derived from it. In consequence the top data point was omitted from one set of analyses for the wet soil first cycle test. Only the five lower strain gauges were employed in the fit as well as the conditions at the pile top and some distance below the lowest strain gauge. The result in terms of the pressure distribution in the pile is shown in Figure 3. Here the fifth-order spline was employed. It can be seen that the removal of the top data point makes the pressure distribution data considerably worse than before in comparison, for example, with Figure 1b. This technique was therefore abandoned.

Finally, as described earlier, the approach was taken of moving the point of zero moment, that is the soil level up and down the pile in order to examine the effect on the pressure distribution. One of the first attempts is shown in Figure 4 where the first cycle of loading in the wet soil was fitted using the assumption that the actual point of load application was five inches below the ground surface formerly assumed. (That is to say, minus 5.0 inches.) As can be seen in Figure 4 this has a distinct effect on the shape of the moment curves introducing at the highest moments some obvious kinks in the moment distribution. The

consequence of these can be noted in Figure 4b where the pressure distributions now assume wild shapes. It was apparent from this experiment that the data were very responsive to changes in the point of zero moment. It seemed worthwhile, therefore, to find out if the pressure distribution assumed a reasonable shape for any point near the assumed value.

In the case of the dry sand data a fifth-order spline was used with zero moment at -0.5 inches, that is half an inch below the originally-assumed ground surface. The results in terms of moment and pressure distribution are shown in Figure 5. This was not considered a satisfactory solution and further attempts were made until eventually what was considered the best result was obtained when zero moment was taken at -0.2 inches; the results are shown in Figure 6. Although the pressure distributions may not as yet be considered perfect, further fitting was terminated at this point in order to examine the pile-soil interaction in more detail. It can be seen that the pressure distributions are considerably improved over those in the original fitting of Figure 1 or in those shown in some of the trials in Figure 5.

Finally, the same process was applied to the data for the first cycle of loading in the wet soil and it was determined that a zero moment located at -0.5 inches achieved the best fit. The results of this analysis in terms of moment distribution and pile-soil interaction pressure are shown in Figure 7. The shapes of the interaction curves in Figure 7b are considered to be the best of those produced in this investigation and seem quite reasonable in terms of the soil-pile behavior. They were therefore used in the further analysis of pile response.

3. Pile-Soil Interaction

3.1 Features of Analysis

From the displacements (not shown) and interaction pressures of Figures 5 through 7, plots can be made of the interaction soil pressure versus pile lateral displacement at various selected depths in the soil. In the pile literature such plots are usually referred to as "p-y" curves with p representing the interaction pressure and y the displacement of the pile. However in the analyses accompanying our reports it is preferred to describe the displacement as u in the more usual coordinate system since it occurs in the coordinate x or horizontal direction. The coordinate z is taken downwards along the axis of the pile. The plots are made by the computer at requested depths. In the preparation of such curves from the computations obviously a great deal depends on the accuracy of the second differentiation. It is felt that the double integration results in a fairly reliable value for displacement at each stage of the test, because the displacement decreases with distance down the pile, the double integration is a fairly good smoothing technique, and the displacement of the top of the pile is known and can be used to check the results of the integration. Less certainty attaches to the values of the soil interaction pressure and they must be assessed by an independent analysis or investigation. A detailed discussion is left for later; the results of the analysis are presented here.

In Figure 8 are shown plots of pressure versus displacement at different depths below ground surface for the dry soil in the first two cycles of loading for the case where the surface was taken at -0.5 inches. These plots therefore correspond to the calculated results displayed in

Figure 5. The depths at which the curves were evaluated were 8, 25, 50, 75, 100, 125 and 150 inches below the surface. In Figure 8a all of the curves are given to indicate the range of results obtained whereas in 8b for clarity only the pressure-displacement curve for a depth of 50 inches is represented.

In order to show the difference which develops as a result of the assumption of the surface level another set of curves is shown in Figure 9. They are again taken from the dry soil test with a surface assumed at a depth of -0.2 inches. In Figure 9a all of the relations are shown and in 9b only the plot for the depth of 50 inches. It can be seen in Figures 8 and 9 that there is little difference in general between the two sets of data except for those at the smaller depths of 8 and 25 inches. This can be confirmed by examining Figures 5b and 6b where it can be seen that the pressure distributions with depth are generally similar except at the upper levels of the pile. Therefore below a depth of a foot or two the assumption as to the surface level is not especially important in the analysis of the data. However, since the behavior of the soil in the top few diameters has most importance for the moments in the pile, it is desirable to utilize the most correct results in analysis. Further analysis for the dry soil will be applied to the case where zero moment was taken at -0.2 inches (Figure 9). In the case of the wet soil the parallel test result is represented in Figure 7 from which the numerical data have been abstracted to give Figure 10. The latter shows the pressure-displacement relations for the soil at the same depths as for the dry sand and when the loading horizon is taken at the depth of -0.5 inches.

3.2 Discussion

On examining the curve of p-u for any depth in Figures 9 and 10 a few points are apparent. The plots exhibit some retrograde behavior at the origin; this is probably a measure of the error in pressure calculations at very low value of loads. Subsequently they follow softening paths as displacement increases. On unloading, the initial route is steep, but it becomes flatter as unloading proceeds. At any depth, when the applied load at ground surface reaches zero again, the interaction pressure is of course nonzero as the pile is held in a deflected position by the soil as a consequence of the plastic strains which have developed. The loading-unloading curves indicate a typical nonlinear soil elastic-plastic behavior. This is more clearly seen in Figure 11 which shows all eight cycles of loading carried out for the 50 inch depth. (The one data point shown well below the others on this figure is a computer error.) The unloading curves are similar to one another and on each reloading cycle the curve rises until it meets the generally plastic upper bound curve of soil deformation. At the shallower depths the soil exhibits larger hysteresis loops than at the greater depths. Almost entirely elastic behavior appears to occur below a depth of between 100 and 125 inches for the dry soil and below 150 inches for the wet soil. It is clearly seen that the stiffness and strength of the soil increases with depth in both materials as expected.

With Figures 9 and 10 plotted to the same scales it can be seen that the resistance of the wet soil at all depths is substantially smaller than that of the dry soil at equivalent depths, because the initial lateral effective stresses in the two cases differ by the product of the unit weight of water and the depth below ground surface. The curves of Figures

9 and 10 can therefore form a basis for various analytical approaches to the problem of soil-pile interaction. This will be discussed in the next section.

One final point should be indicated. The saturated soil p-u curves appear quite reasonable, as they are presented in Figure 10. At the smaller depths, the response, both elastic and plastic, is soft, the displacements are large, and the interaction pressures low. As the depth increases, the response becomes stiffer, and the peaks occur at smaller displacements and higher pressures. However, at the greater depths, although the soil stiffness increases, the deflections are no longer large enough to generate higher pressures, so that the peak pressures occur at about 50 to 75 inches depth. The response curves at greater depth follow in logical order, except for that at 100 inches, of increasing stiffness and diminishing displacement and pressure. This succession is not followed in the dry soil p-u curves, Figure 9, as a result of the cumulative errors in the analysis process. The curves at successive depths do exhibit the characteristics of increasing stiffness, declining displacements, and increasing then decreasing peak pressures. However, apparently because of relatively displaced origins, the plots tend to overlap, with those for 100, 125 and 150 falling logically with respect to each other, but inside the 75 inch curve. An improvement would be effected by moving the origins of the 50 and 75 curves some distance to the right on the figures. This has not been done, and the figures are shown as they were produced from the computer. The slopes used in the analyses are taken directly from the data in Figures 9 and 10.

4. Approaches to Fitting p-u Curves

4.1 Discussion

It is apparent from Figures 9 and 10 that an elastic-perfectly plastic model does not fit the behavior of the soil at any of the depth ranges. This might be expected since the pressure caused by a lateral movement of a segment of pile at depth in sand would not be expected to reach an asymptotic value. Greater displacements are accompanied by increased resistance even after yielding develops in the soil. An exact analysis of the displacement of a rigid circular or square segment of pile in an elastic-plastic medium has not been accomplished. The nearest analysis for which an analytical result is available is that of the expansion of a cylindrical cavity in a plain strain in an elastic plastic medium. Although it may be possible to adapt this solution to the present case, initial attempts indicate that the expanding cavity system may be too stiff in comparison with the laterally-displacing pile. Appendix A gives the relationships derived. For the problem of a solid-rigid cylinder displaced laterally in a linearly-elastic medium under plane-strain conditions, a solution has been obtained and will be given in a later report. This problem does not seem to have been solved before.

Since in evaluation of the pile-soil interaction, a tortuous path is followed, involving data generation (strain gauges) at 100g, amplification and transmission through slip rings to signal conditioners, recording on the Honeywell, calibration, digitization and finally double differentiation and integration, a reasonable question to ask is: how good a picture is the final result of pile reaction pressure versus displacement? Rather than performing a step-by-step sensitivity analysis, it seemed more practical to

adopt another procedure. In this, the same pile as before is imbedded in a supporting system of linear springs thus approximating very closely the Winkler foundation. When this arrangement is set up so that the data from a lateral load test at 1g are transmitted through the centrifuge system (amplifiers, sliprings, etc. to the recorder) and then digitized and processed as before, the final result of pile pressure versus deflection at any point on the pile can be compared with the precisely-known, linear, and reversible spring constant. The scatter or divergence of the final calculated result will indicate the reliability of the results from the soil test, except for the 100g conditions of the latter experiment. Two tests of this "Winkler" foundation have been attempted to date, but difficulties were encountered in selecting a desirable spring constant to be fairly close to the indicated soil resistance and in establishing proper boundary conditions for the test and analysis. When the tests are completed in the near future, the results will be reported.

With the assumption for the present, that the pile-soil test results are a reasonable representation of the nature of the lateral interaction between pile and soil, further analysis of these curves has been done and is described below.

Examination of the pressure-displacement curves of Figures 9 and 10 shows that there is no horizontal asymptote to the pressure at any depth in the soil. A reasonable characterization of the behavior would be one of a bilinear representation. Here the pile pressure-displacement relation is linear up to a point ("yield") and continues linear but at a different slope beyond that point. The unloading curve can also be taken as a straight line.

A suggested straight line fit to the data at 50 inches depth in the dry soil of Figure 9(b) is shown. With this characterization it is possible to describe the variation of the slopes of the lines as a function of depth in the soil purely empirically, without regard to any model of soil response; this has been attempted as described in the following section.

4.2 Parameter Variations with Depth

Examination of Figures 9 and 10 reveals a number of points: (1) a bilinear characterization is reasonable; (2) the initial stage of each unloading path can be taken as parallel to the straight line describing the first response to load; (3) the initial loading straight line becomes steeper with depth from the surface; (4) the intersection of the two straight lines occurs at a higher pressure with depth; (5) the intersection becomes harder to discern at depth so that a single linear characterization may be more valid beyond a depth depending on the load level; (6) the dry soil is stiffer than the saturated soil; (7) for loading only, a linear function would describe the soil behavior reasonably well, better in the saturated sand case than for dry sand. A number of these features have been examined.

For convenience, the slope of the pressure versus displacement (p-u) curve during initial loading is designated as k^e, which is also used to describe the average slope of an unloading-loading curve. The slope of the second, plastic portion of the bilinear function is assigned the symbol k^p. At a pressure of p^*, and displacement u^*, the two lines intersect. At greater depths, p^* and u^* can usually not be distinguished. It is assumed therefore that a particular loading will cause the soil to yield around the pile down to a particular depth; below that depth the soil response is

elastic, and is assumed to be linearly elastic herein. The yield pressure p^*, elastic modulus k^e, and yield displacement u^* are related by the expression

$$u^* = \frac{p^*}{k^e} \qquad (4.2.1)$$

To avoid too much bias in the interpretation of the tests, the pile pressure-displacement data were analyzed by three people, two of whom had no preconceived opinions about the relations between the variables. They were given the task of judging values of k^e, k^p and p^* by eye for each curve corresponding to a given depth. Since both wet and dry saturated sands could be taken plausibly to have no strength at ground surface it was decided to assume a parameter-depth relation in power form as

$$k^e = C^e(\gamma' z)^{\ell} \quad ; \quad k^p = C^p(\gamma' z)^m \quad ; \quad p^* = C^*(\gamma' z)^n \qquad (4.2.2)$$

The values selected to fit the pressure-displacement curves were then employed in a computer program to determine by least squares fitting, the best values of C^e, C^p, C^*, ℓ, m, and u suiting the data. In these expressions (4.2.2), the term γ' is the effective unit weight of the soil, equal to the total unit weight for the dry soil and the buoyant unit weight for the wet; z is the depth.

4.2.1 Dry Sand Test

After comparison of the three sets of calculated data the values determined are given in Table 4.2.1.1. It was not initially presumed that u^* would follow equation (4.2.1), so that p^* and u^* were found independently.

TABLE 4.2.1.1 DRY SAND

Effective Vertical Stress, psi	Depth in	k^e psi	k^p psi	p* lb/in	u* in
0.449	8	110	55	16	0.125
1.403	25	900	500	80	0.075
2.807	50	4,100	1,200	300	0.067
4.210	75	8,000	1,900	450	0.055
5.613	100	10,500	2,100	[600]	[0.034]
7.017	125	15,000	[3,100]	-	-
8.420	150	20,500	[6,000]	-	-

The blanks in the table refer to points where the parameter in question could not be discerned. It appears that the soil behavior below a depth of 75 to 100 inches for this load range is elastic.

Values of the exponents in equations (4.2.2) from the computer statistics were:

$$\ell = 1.792 \; ; \; m = 1.466 \; ; \; n = 1.480 \; ; \; \text{exponent for } u^* = -0.444 \qquad (4.2.1.1)$$

The correlation coefficients were respectively 0.997, 0.988, 0.996 and 0.947. From equation (4.2.1), therefore

$$u^* = \frac{p^*}{k^e} = \frac{z^{1.480}}{z^{1.792}} = z^{-0.312} \qquad (4.2.1.2)$$

The constants were $C^e = 508$; $C^p = 221$; $C^* = 53$; $C^u = 0.091$.

Further discussion is postponed until the saturated sand results have been presented.

4.2.2 Saturated Sand Test

The results from analysis of Figure 10 are given in Table 4.2.2.1.

TABLE 4.2.2.1 SATURATED SAND

Effective Vertical Stress, psi	Depth in	k^e psi	k^p psi	p* lb/in	u* in
0.277	8	190	100	26	0.15
0.865	25	1,100	350	70	0.068
1.730	50	1,800	800	105	0.058
2.595	75	2,500	950	116	0.045
3.461	100	3,200	[1,050]	[80]	[0.025]
4.326	125	4,700	1,200	122	0.025
5.191	150	7,700	1,600	132	0.015

Square brackets indicate dubious results. In this case the soil behavior evidently extended into the plastic range for the maximum loads applied at all depths, although plastic behavior appears marginal at the 150 inch level.

The results of k^e and k^p for both dry and saturated sand are plotted in Figure 12 versus vertical effective stress. No statistical analysis of the wet sand tests is given for the reason explained below.

4.2.3 Discussion of Results

When the statistically-evaluated curves of equations (4.2.1.1) and (4.2.1.2) for the dry test are compared with the plotted points in

Figure 12, it is apparent that, although they fit the data quite well, as good a fit can be obtained by a curve selected by hand. The two computed curves are shown in Figure 12 as well as two hand-drawn functions

$$k^e = 817.6(\sigma_z')^{1.5} \qquad (4.2.3.1)$$

for the elastic response, and

$$k^p = 350\sigma_z' \qquad (4.2.3.2)$$

for the plastic behavior.

The first of these was intended to account for only the dry test data, but it provides a reasonable fit for the saturated sand test as well, although the latter exhibit more scatter. Since, as indicated rationally in Appendix A, or otherwise, the value of k^e is a multiple of the shearing modulus of sand, it follows that this soil modulus also increases with depth to a power of about 1.5. Commonly, it has been found (4 , 8) that shear modulus increases with confining pressure only to about the one-third or one-half power in sands; the higher power demonstrated here (if not due to a test or interpretation error) is a consequence of the three-dimensional nature of the actual test. Near the surface, the soil is unconfined and moves upwards to the free surface out of the way of the deflecting pile. The near surface modulus is therefore apparently lower than would be expected. With depth, the laterally-moving pile and soil more closely conform to a plane-strain system, and the modulus increases. The observed effect in the surface regions is therefore of a "modulus" increasing rapidly with depth. Were the deflections of the pile greater at depths, it is possible that the observed behavior might follow a function closer to the one-half power of depth.

On examining the dry sand plastic modulus k^p in Figure 12, it is seen that it is more erratic than k^e and although the function from the constants and equation (4.2.1.1) fits it fairly well, scatter is evident. Adding in the wet sand data, it appears that the dry and wet points are reasonably consistent if a straight line fit, equation (4.2.3.2), is employed. There is enough scatter in the p* points that it was not felt to be worthwhile to plot them in Figure 12. They would fit a straight line as well as any other function, and this would then, by equation (4.2.1) indicate a -0.5 power dependence of u* on depth.

Some attempt can be made to fit the test information to the framework of the theory of Appendix A. First of all, it is desirable to get a feel for the behavior of equation (A.1.12). It is plotted in Figure 13.

For a value of p_0', corresponding to a depth of 75 inches in the saturated sand, and an at-rest earth pressure coefficient of 0.7, as well as an arbitrary value of G, Figure 13 shows the variation of resistance with displacement for a range of ϕ from 30° to 50°. In contrast to the vertical bearing capacity problem, where the gravity gradient is important, the pressure is not very sensitive to the friction angle. The plotted points are those obtained from the computed results at a depth of 75 inches in the saturated sand. It is seen that they are substantially higher than the curves obtained from equation (A.1.12).

In order to achieve a better fit, the only parameters that effectively can be changed are G and p_0', although the lateral at-rest soil pressure p_0' is constrained by the depth and the range of possible values of lateral earth pressure coefficient (which could be as high as the passive

earth pressure coefficient, equal to about six for a friction angle of 45°). In a further comparison, G was increased to give a soil reaction pressure versus displacement curve which better matched the 75-inch depth saturated sand data. The result is shown in Figure 14, where G was taken to be 1,333 psi, and ϕ equal to 45°. This is felt to be too high for G for sand at the depth in question. Applying equation (A.1.10) to the data in Table 4.2.2.1 at 75 inches gives G to be $k^e/8$ or 2,500/8 = 333 psi which is a plausible value for the saturated sand. When this value is used in equation (A.1.12) it is necessary to raise the value of p_0' in order to obtain identification with the test results. A trial is shown in Figure 14, in which p_0' was taken to be twice the value of vertical effective stress at 75 inches depth in the saturated sand, or 5.19 psi. This therefore corresponds to a horizontal earth pressure coefficient of 2 before the test began. Such a value might be consistent with lateral displacement of the soil as a result of pile placement, but is higher than is normally considered to act. The comparison with the 75 inch test result is fair.

5. References

1. Ahlberg, J.H., Nilson, E.N., and J.L. Walsh, "Theory of Splines and Their Applications," Section 5.7, p. 560 ff, Academic Press, 1967.

2. Cox, W.R., Reese, L.C. and B.R. Grubbs, "Field Testing of Laterally Loaded Piles in Sand," Proc. 6th Am. Offshore Technology Conf., Paper No. OTC 2079, Houston, Texas, May 1974.

3. Gibson, R.E., and W.F. Anderson, "In-Situ Measurement of Soil Properties with the Pressuremeter," Civil Engineering and Public Works Review, 56, No. 658, pp. 615-618, May 1961.

4. Hardin, B.O., and V.P. Drnevich, "Shear Modulus and Damping in Soils: I. Measurement and Parameter Effects, II. Design Equations and Curves," Tech. Reps. UKY 27-70-CE 2 and 3, Univ. of Kentucky, July 1970.

5. Reese, L.C., Cox, W.R., and F.D. Koop, "Analysis of Laterally Loaded Piles in Sand," Proc. 6th Am. Offshore Technology Conf., Paper No. OTC 2080, Houston, Texas, May 1974.

6. Scott, R.F., "Centrifuge Studies of Cyclic Lateral Load - Displacement Behavior of Single Piles," Final Report 1976-1977 Research Program for API OSAPR Project 8, Calif. Inst. Tech., December 1977.

7. Scott, R.F., "Centrifuge Studies of Cyclic Lateral Load - Displacement Behavior of Single Piles," Report through May 30, 1978 on Research Program for API OSAPR Project 8, Calif. Inst. Tech., June 1978.

8. Seed, H.B. and I.M. Idriss, "Soil Moduli and Damping Factors for Dynamic Response Analysis," Univ. Calif. Berkeley, Earthquake Engineering Research Center, EERC 70-10, December 1970.

6. Acknowledgements

John Lee built the apparatus and performed the tests analyzed here. Some of the analysis was done by M. J. Craig. J.-P. Bardet assisted in verifying and carried out calculations of the work in Appendix A. The report was typed by Mrs. G. Jackson.

FIGURE CAPTIONS

Figure No.	Caption
1	Soil interaction pressure versus depth (7): (a) Dry soil; (b) Saturated soil.
2	Cubic spline fit first loading cycle, dry soil: (a) Moment curves; (b) Soil pressure distribution.
3	Fifth order split fit, first loading cycle, saturated soil; top strain gauge data point removed: (a) Moments; (b) Pressure distribution.
4	First loading cycle, saturated soil, loading point at -5.0 inches: (a) Moments; (b) Pressures.
5	First loading cycle, dry soil, loading point at -0.5 inches: (a) Moments; (b) Pressures.
6	First loading cycle, dry soil, loading point at -0.2 inches: (a) Moments; (b) Pressures.
7	First loading cycle, saturated soil, loading point at -0.5 inches: (a) Moments; (b) Pressures.
8	Two loading cycles, dry soil, loading point at -0.5 inches soil interaction pressure versus displacement as a function of depth: (a) All depths; (b) 50 inch depth only.
9	Two loading cycles, dry soil, loading point at -0.2 inches, pressure versus displacement as a function of depth: (a) All depths; (b) 50 inch depth only.
10	Two loading cycles, saturated soil, loading point at -0.5 inches, pressure versus displacement as a function of depth: (a) All depths; (b) 50 inch depth only.
11	Dry soil, loading point at -0.2 inches; pressure versus displacement at 50 inch depth for all 8 loading cycles.
12	Dry and saturated soils, elastic and plastic moduli versus vertical effective stress, and fitting curves: $A - k^e = 508(\sigma_z')^{1.792}$; $B - k^e = 818(\sigma_z')^{1.5}$; $C - k^p = 221(\sigma_z')^{1.466}$; $D - k^p = 350\sigma_z'$ Values in pounds per square inch (psi).

FIGURE CAPTIONS (CONT'D)

Figure No.	Caption
13	Equation (A.1.12) for soil/pile interaction force per unit of pile length versus displacement for selected values of parameters, and range of friction angles (PHI). Plotted points are test results for saturated soil, 75 inch depth.
14	Equation (A.1.12) for soil/pile interaction force per unit of pile length versus displacement for selected values of parameters. Plotted points are test results for saturated soil, 75 inch depth.
A.1	Approximate analysis for lateral pile displacement in plane strain: (a) Static effective stress on pile; (b) Effective pressure redistribution when pile displaced distance u; (c) Approximation when right side of pile expands radius by u, left side contracts radius by -u.

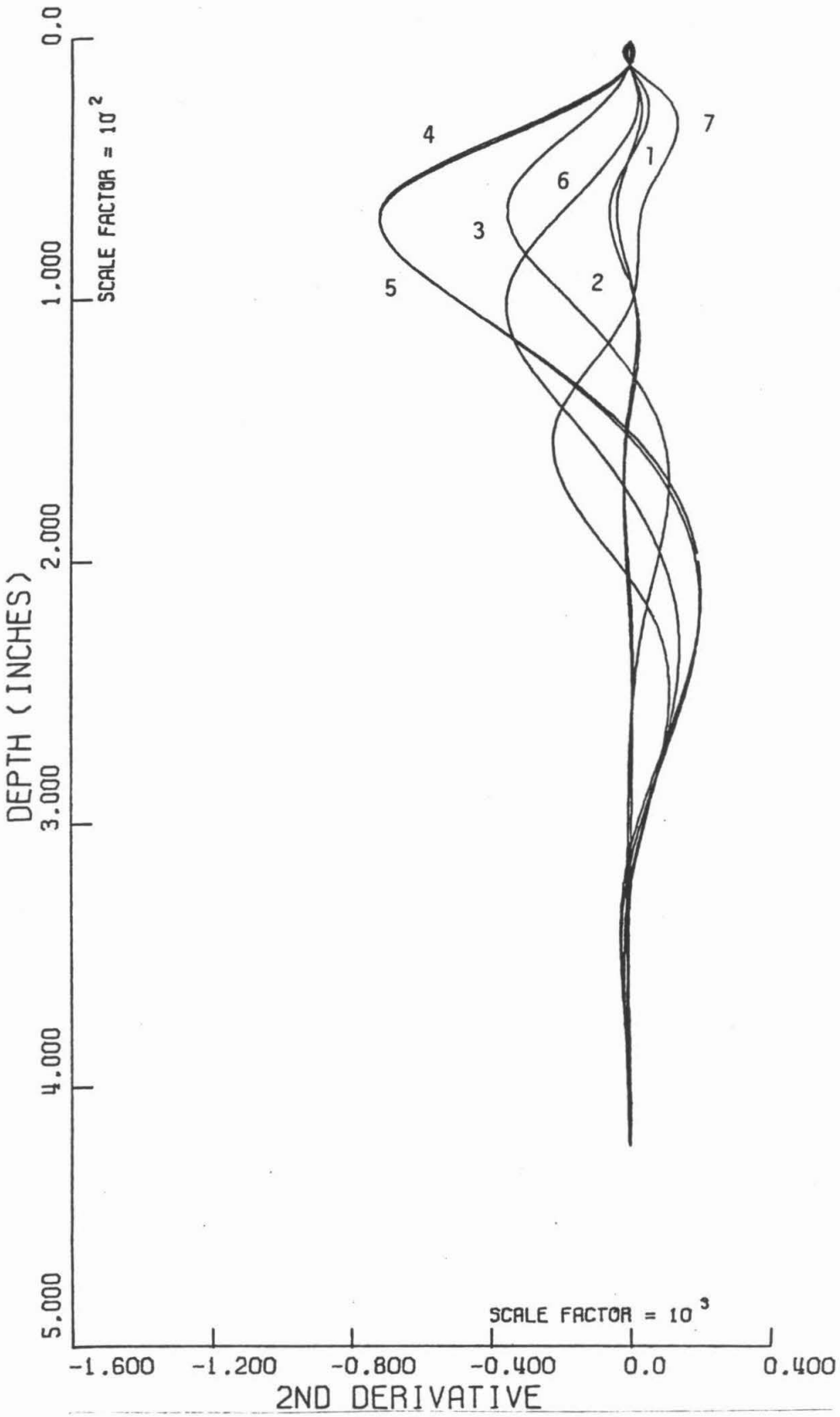

Fig. 1 Soil interaction pressure versus depth (7): (a) Dry soil

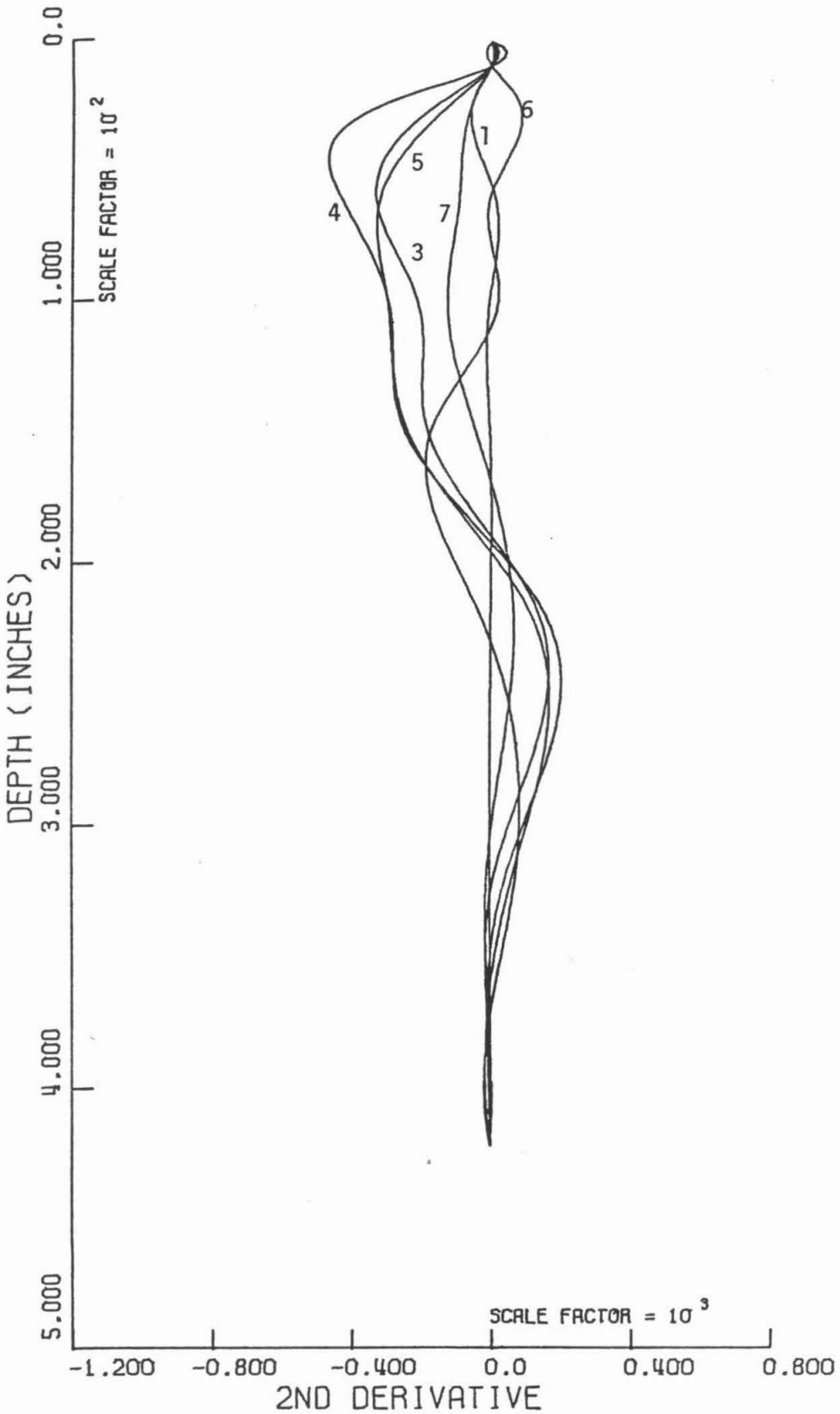

Fig. 1(b) Saturated soil.

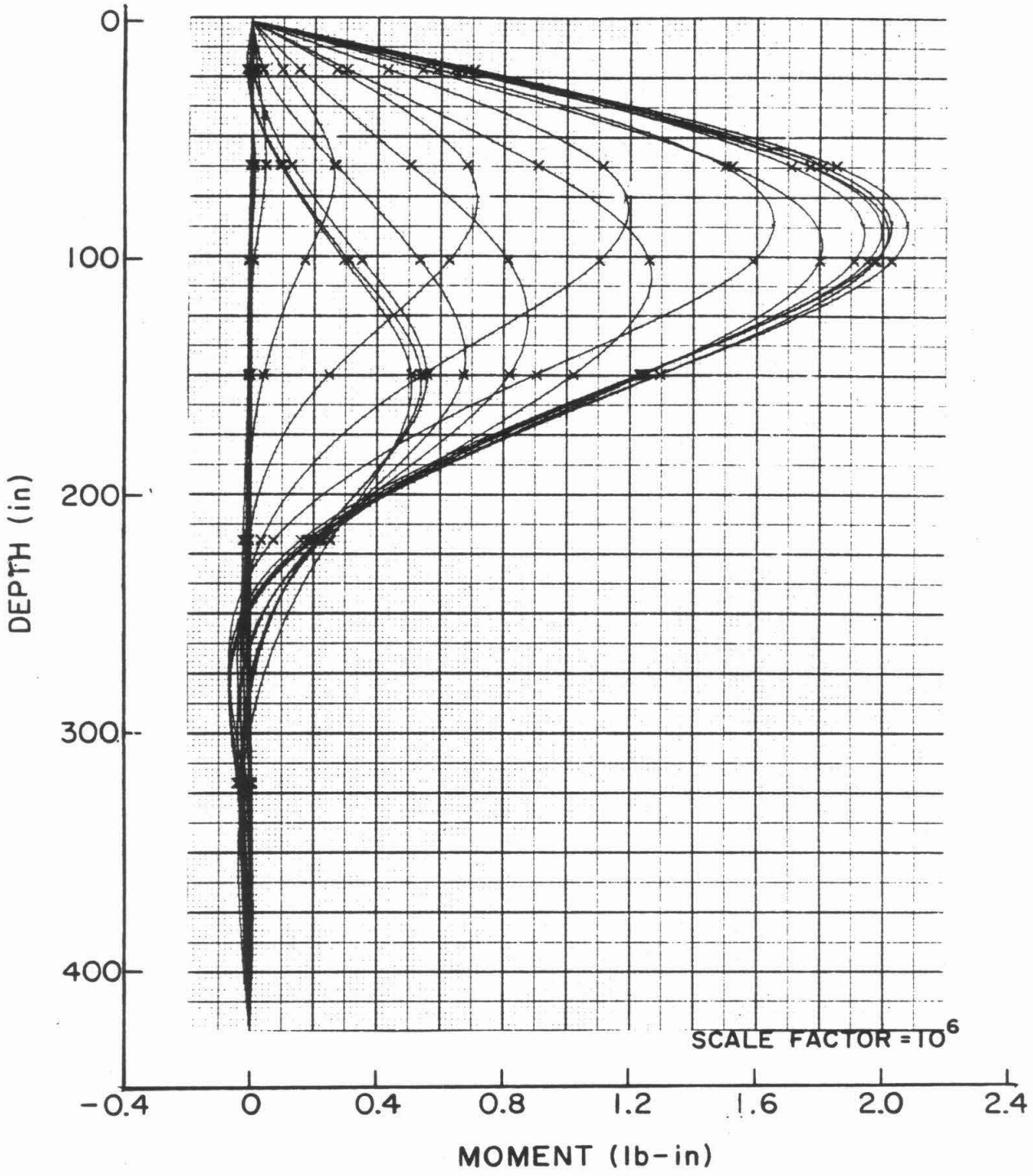

Fig. 2 Cubic spline fit first loading cycle, dry soil:
(a) Moment curves.

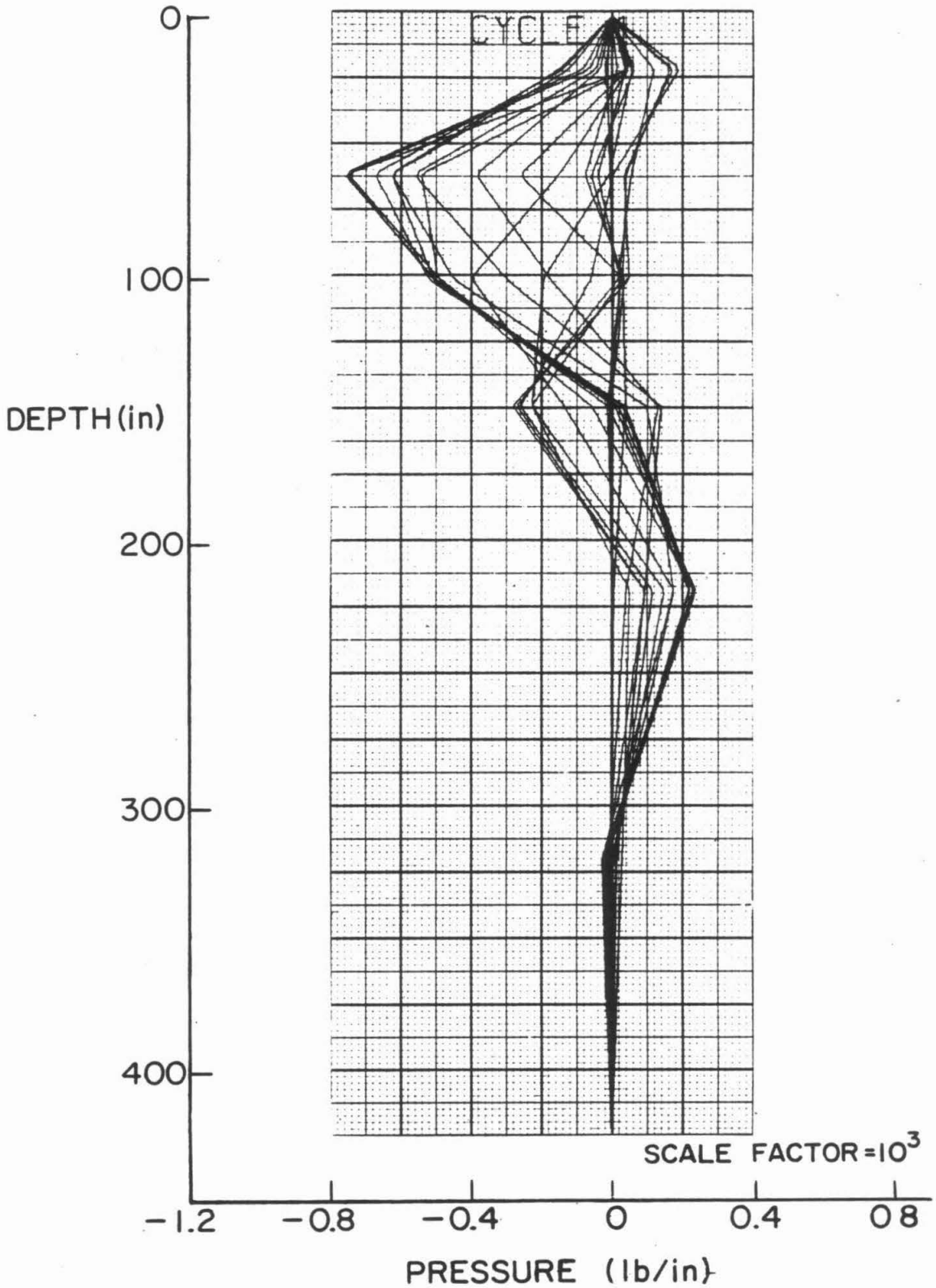

Fig. 2(b) Soil pressure distribution.

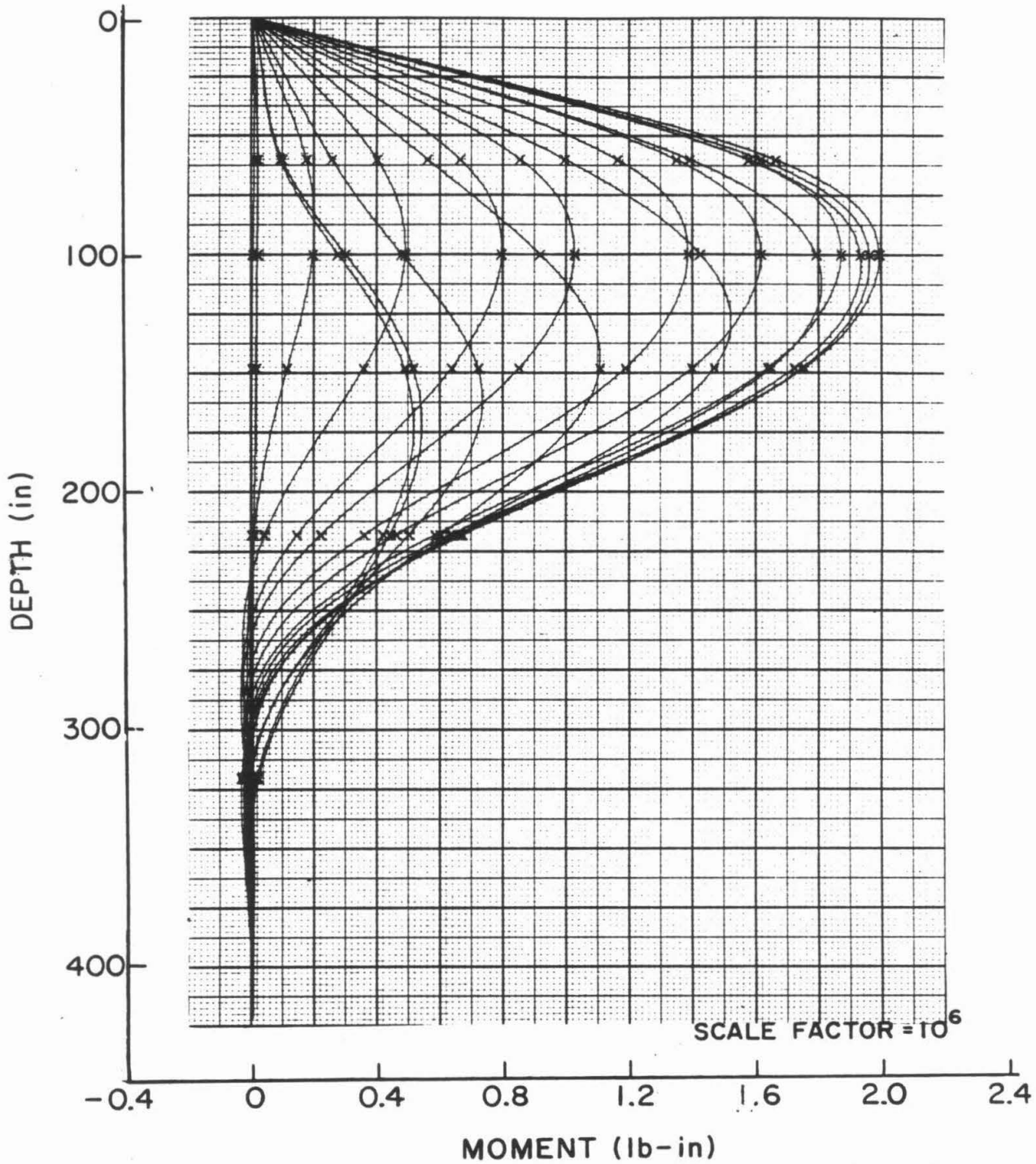

Fig. 3 Fifth order split fit, first loading cycle, saturated soil; top strain gauge data point removed:

(a) Moments.

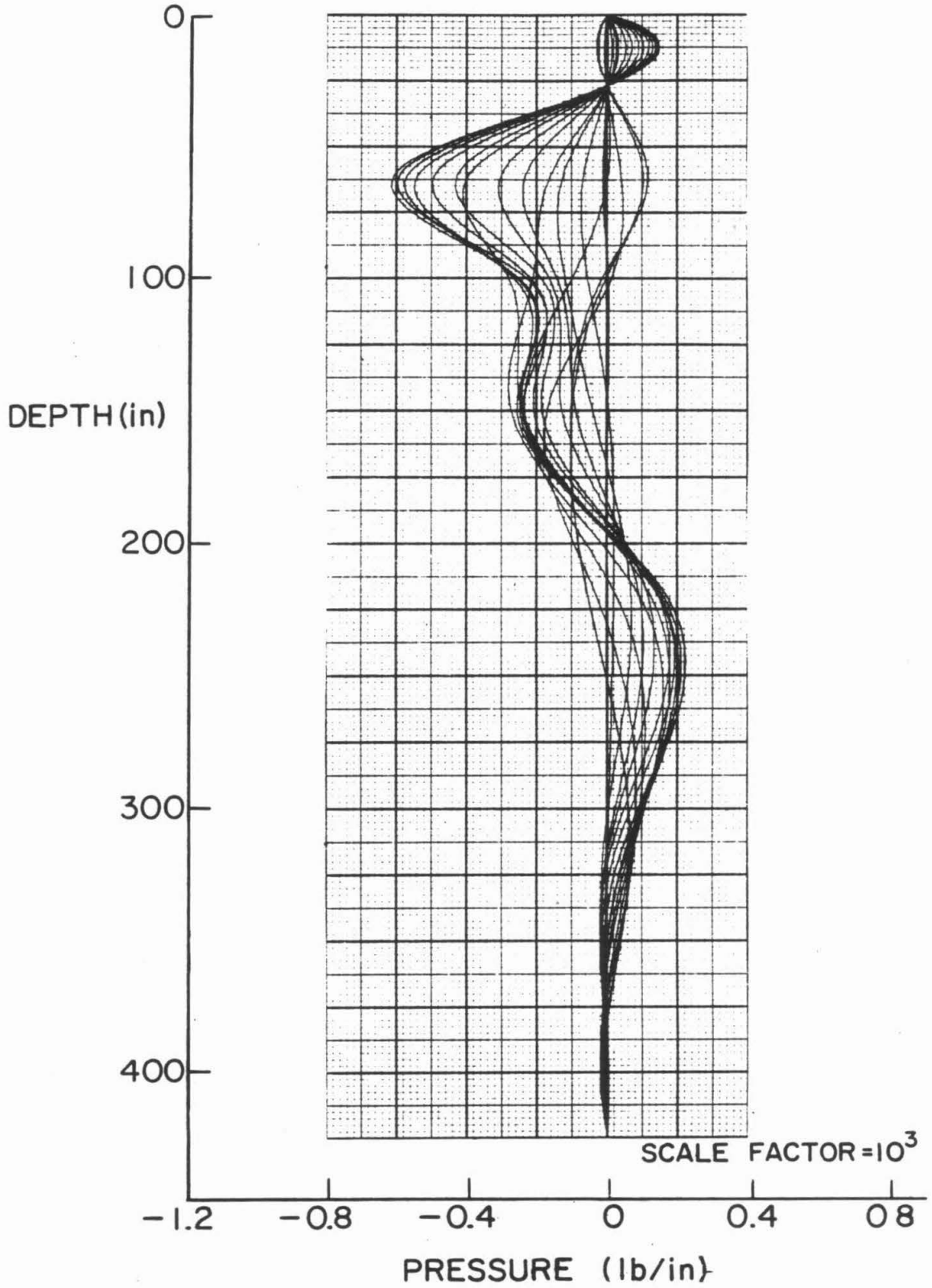

Fig. 3(b) Pressure distribution.

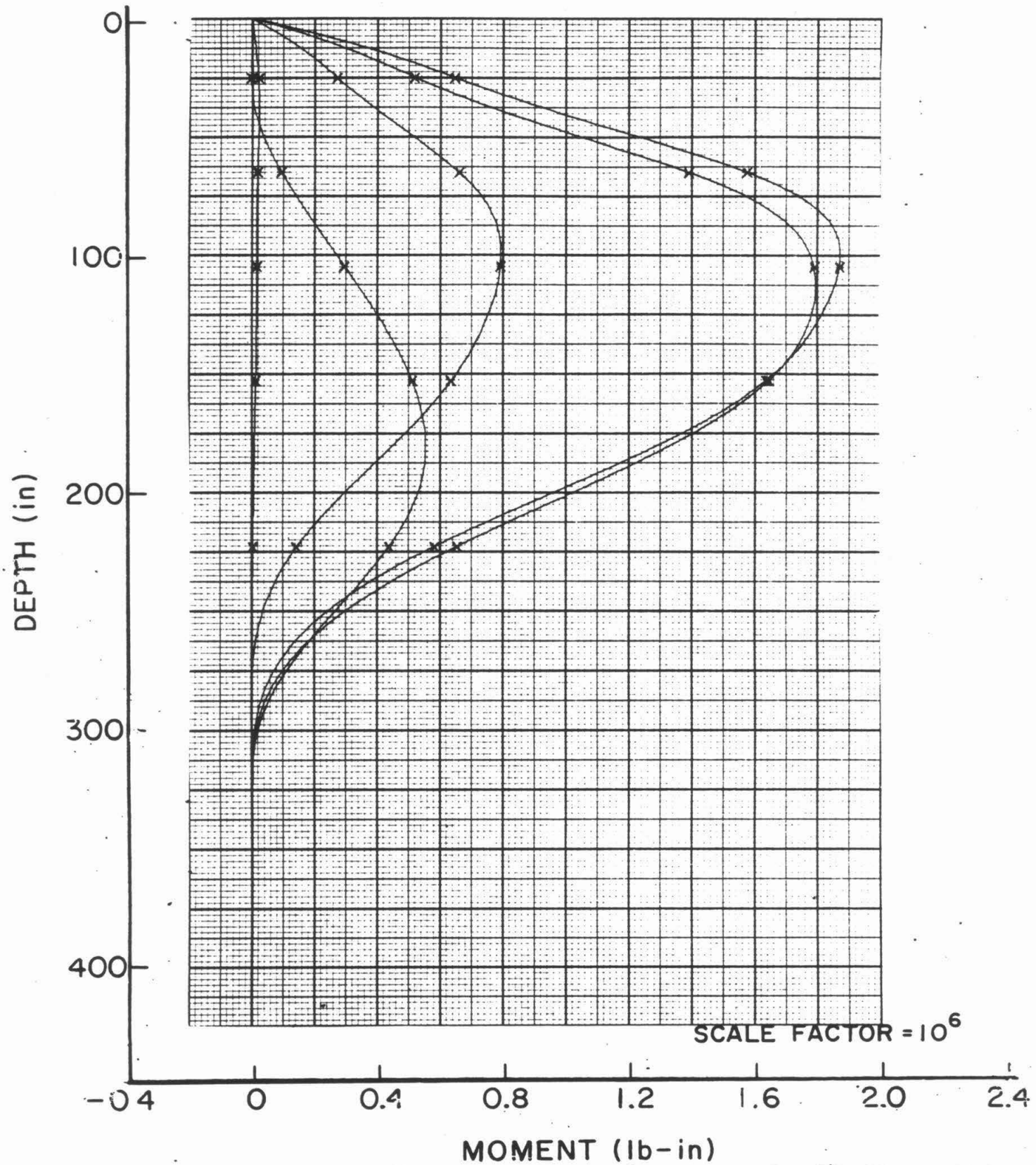

Fig. 4 First loading cycle, saturated soil, loading point at -5.0 inches: (a) Moments.

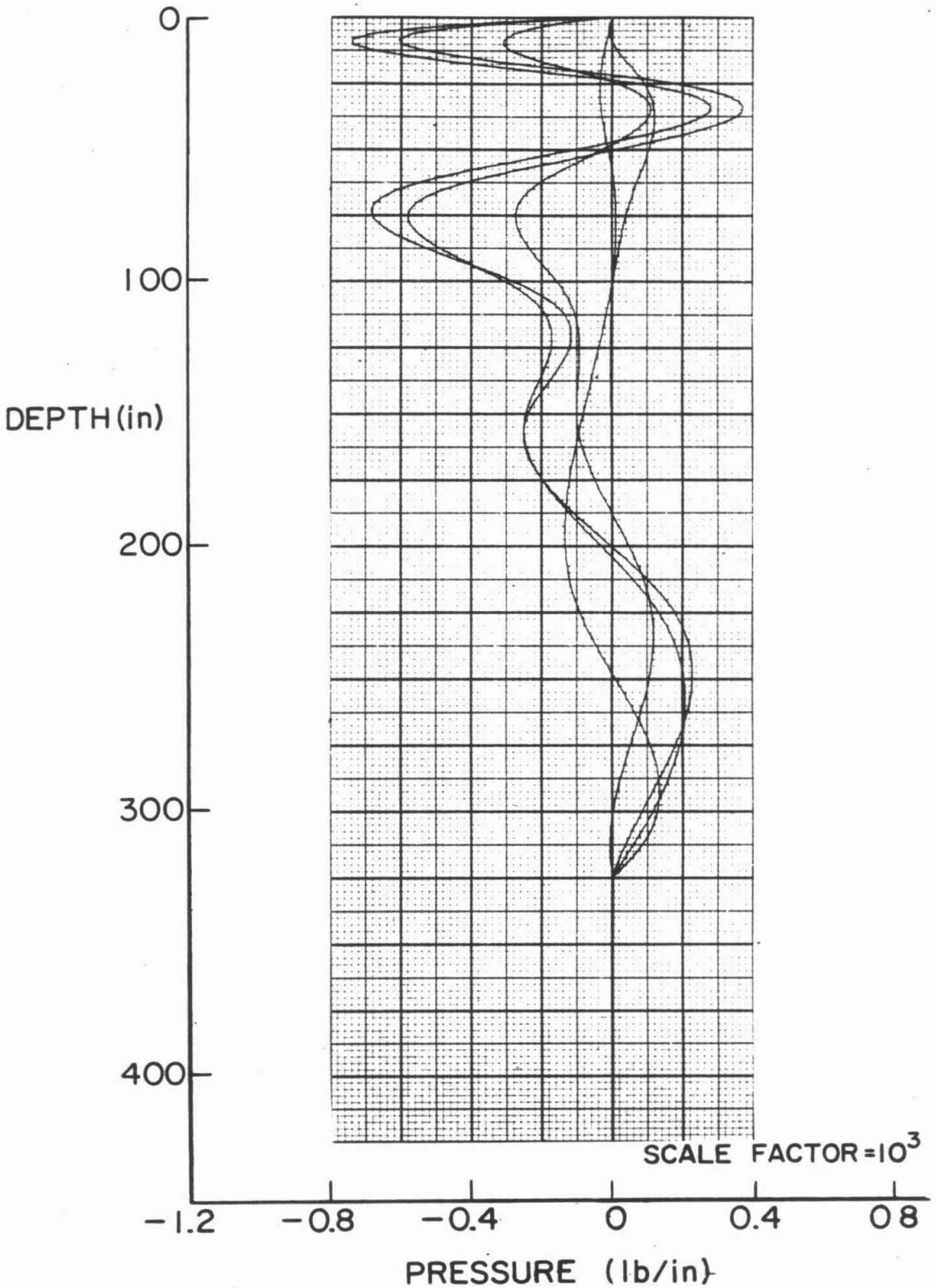

Fig. 4(b) Pressures.

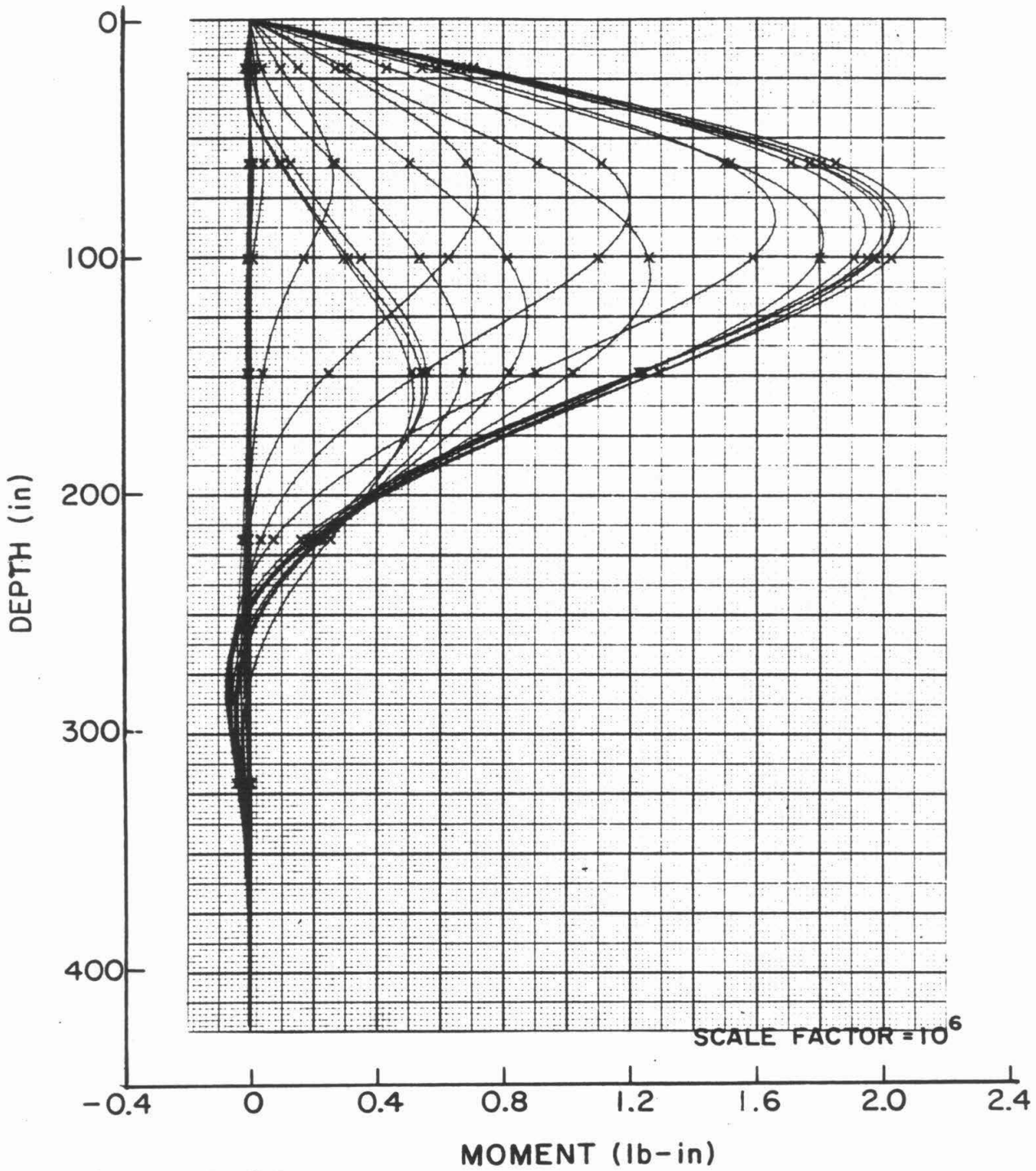

Fig. 5 First loading cycle, dry soil, loading point at -0.5 inches: (a) Moments.

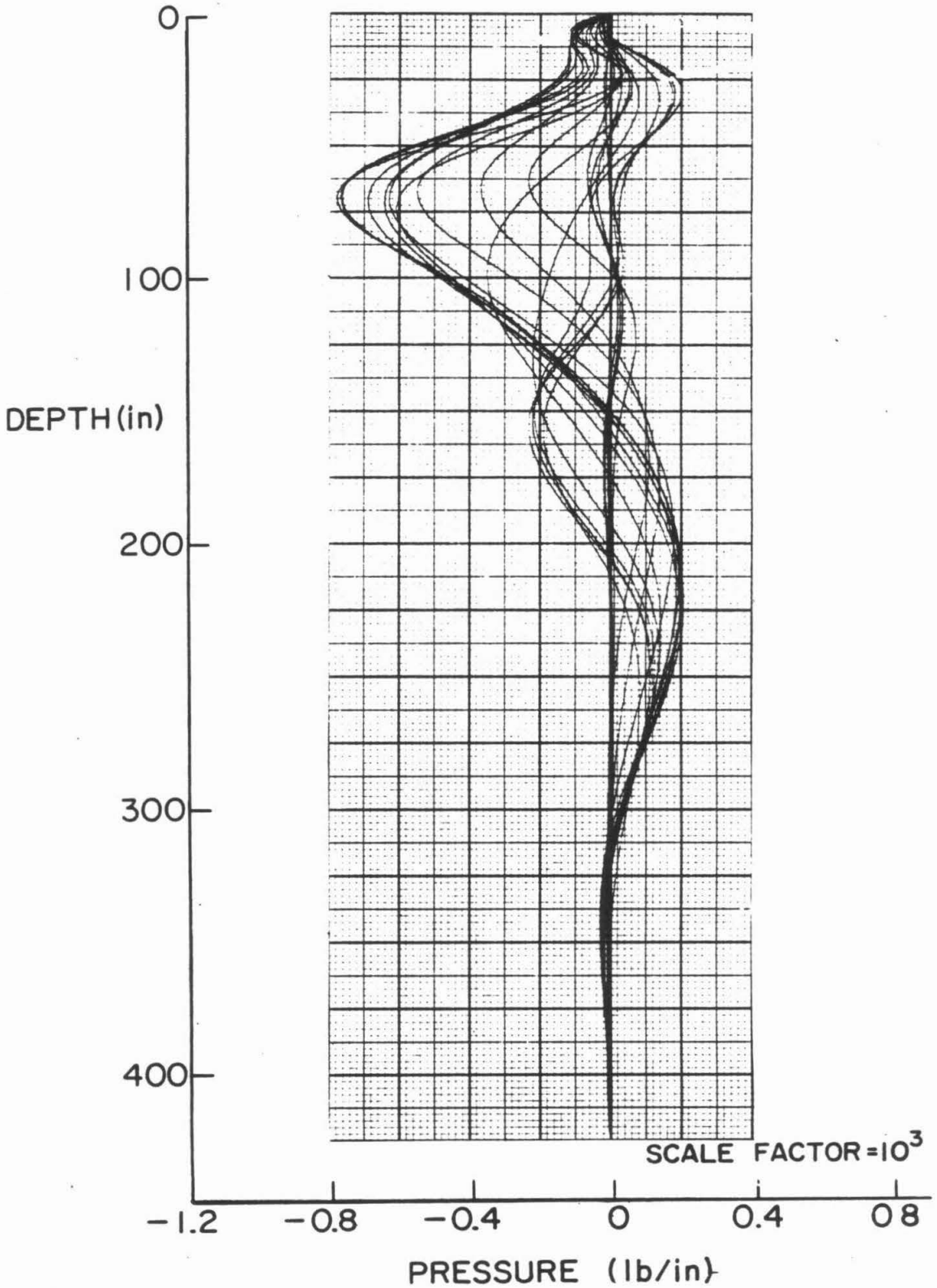

Fig. 5(b) Pressures.

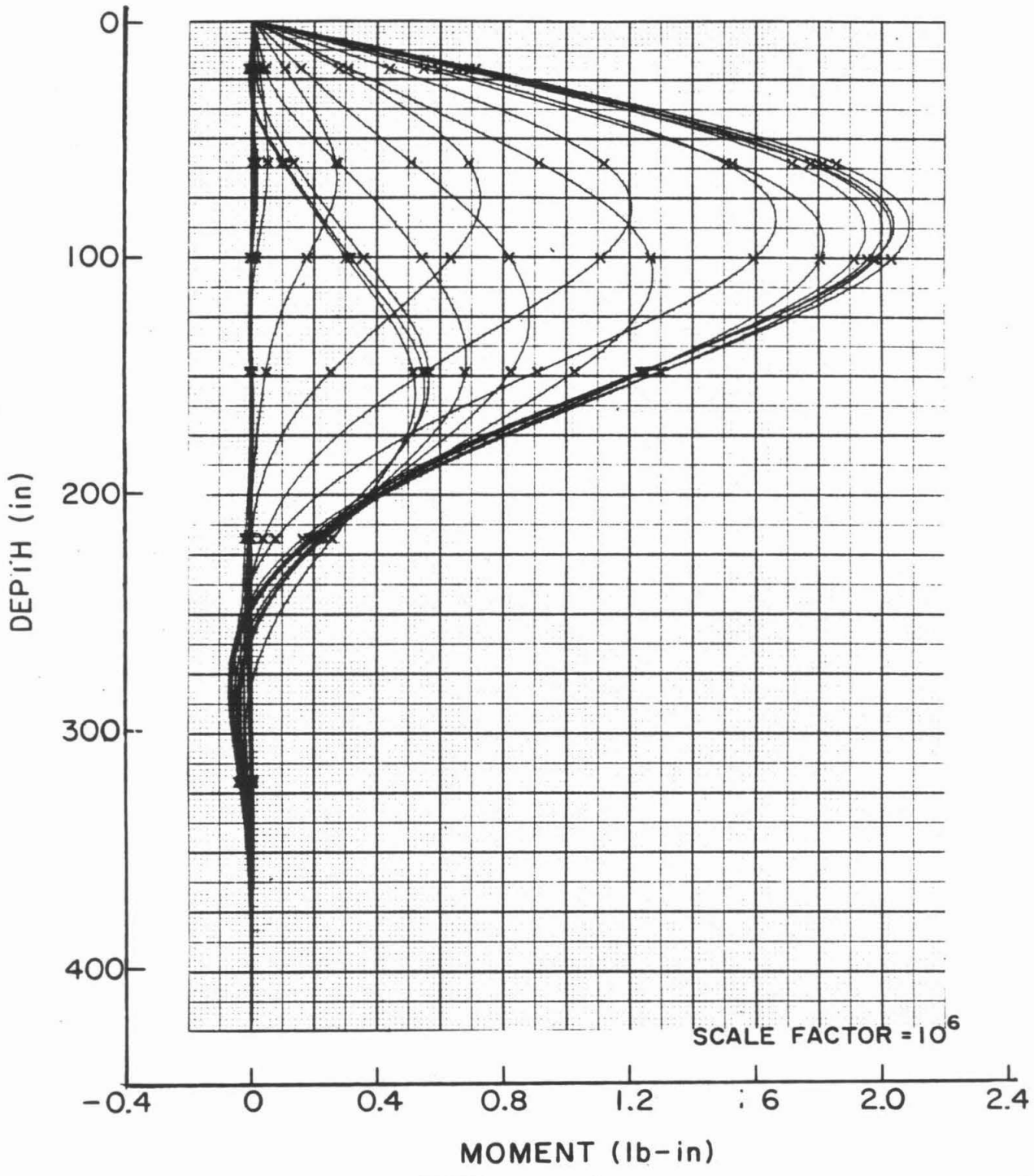

Fig. 6 First loading cycle, dry soil, loading point at -0.2 inches: (a) Moments.

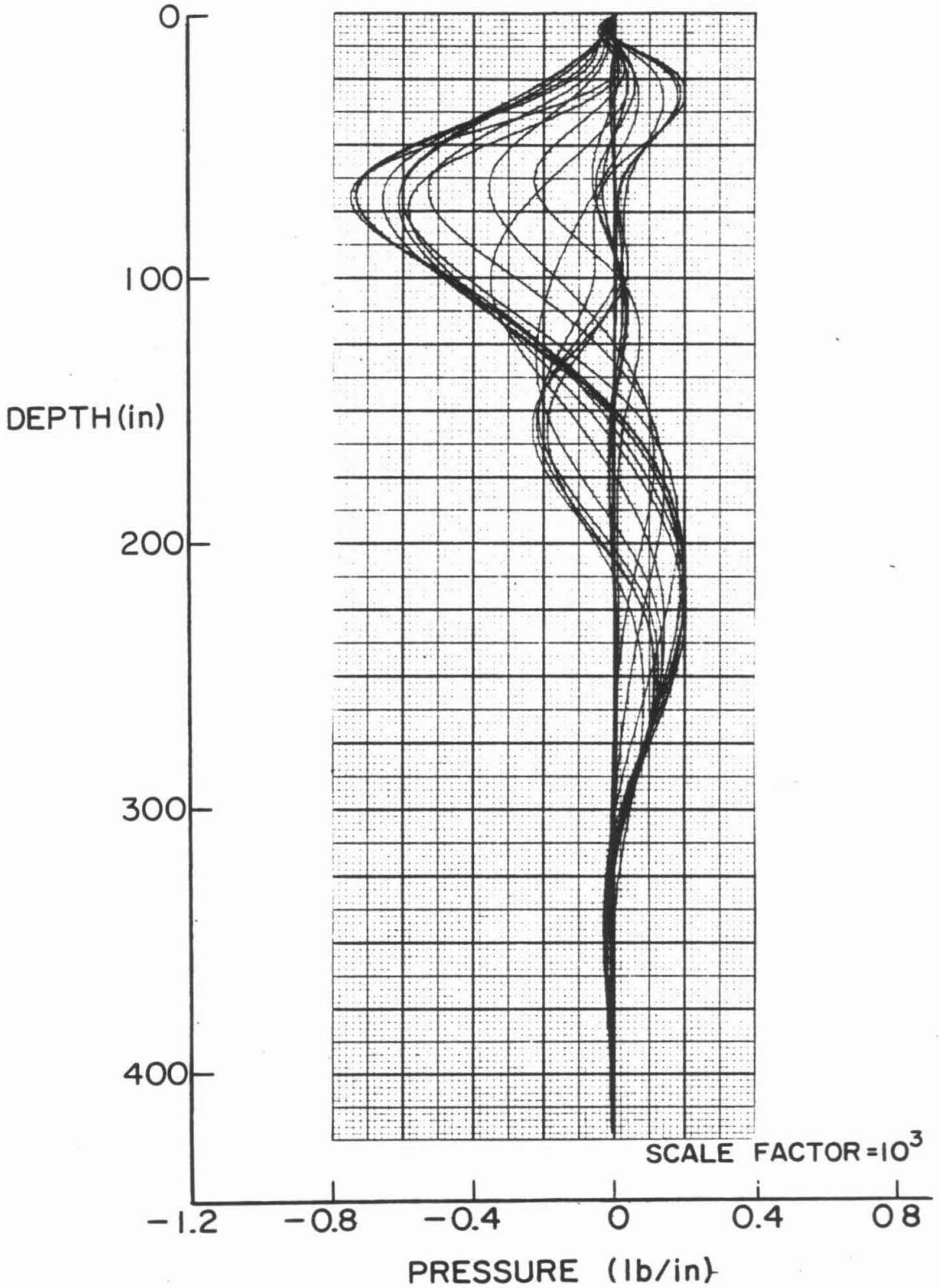

Fig. 6(b) Pressures.

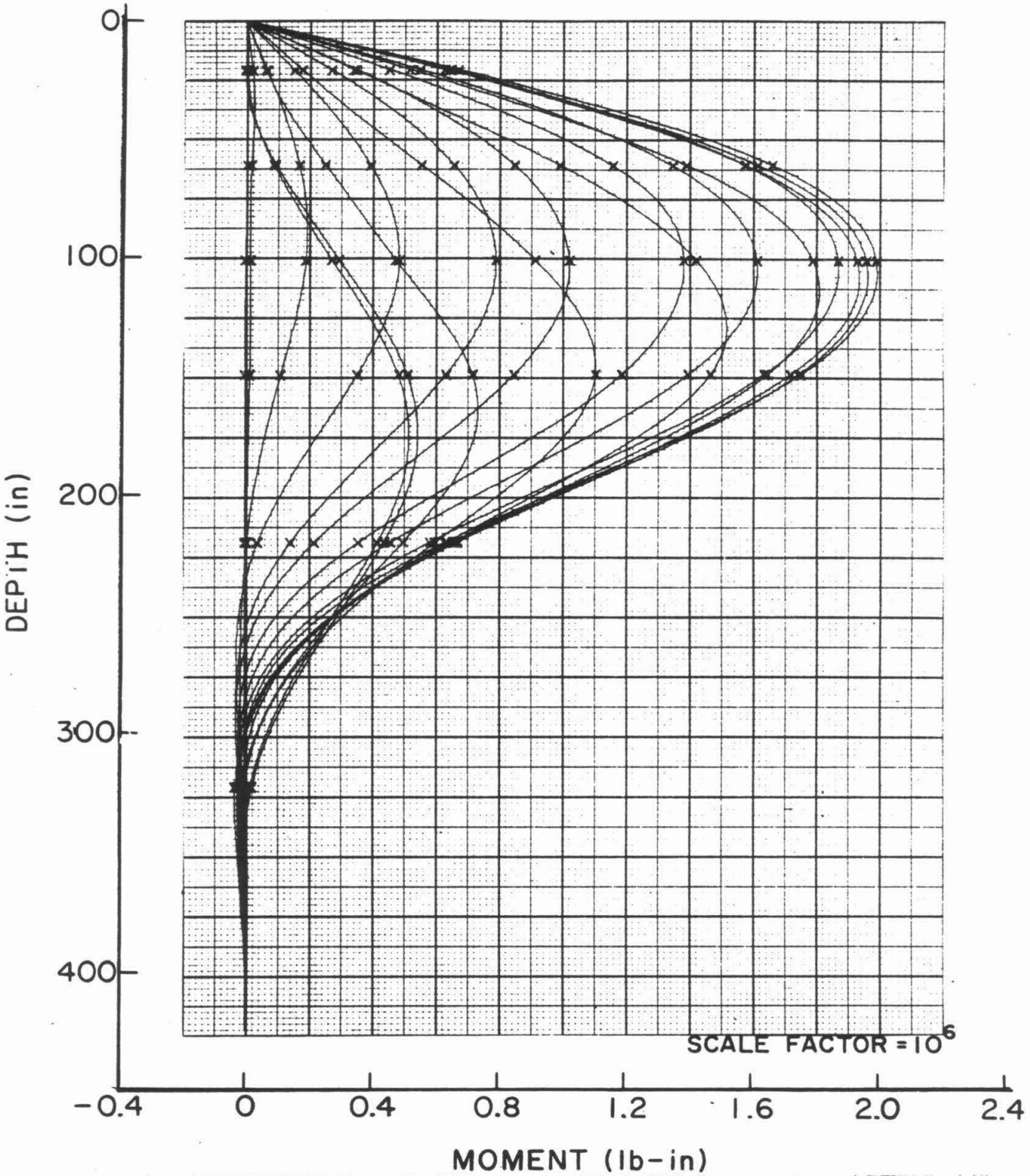

Fig. 7 First loading cycle, saturated soil, loading point at -0.5 inches: (a) Moments.

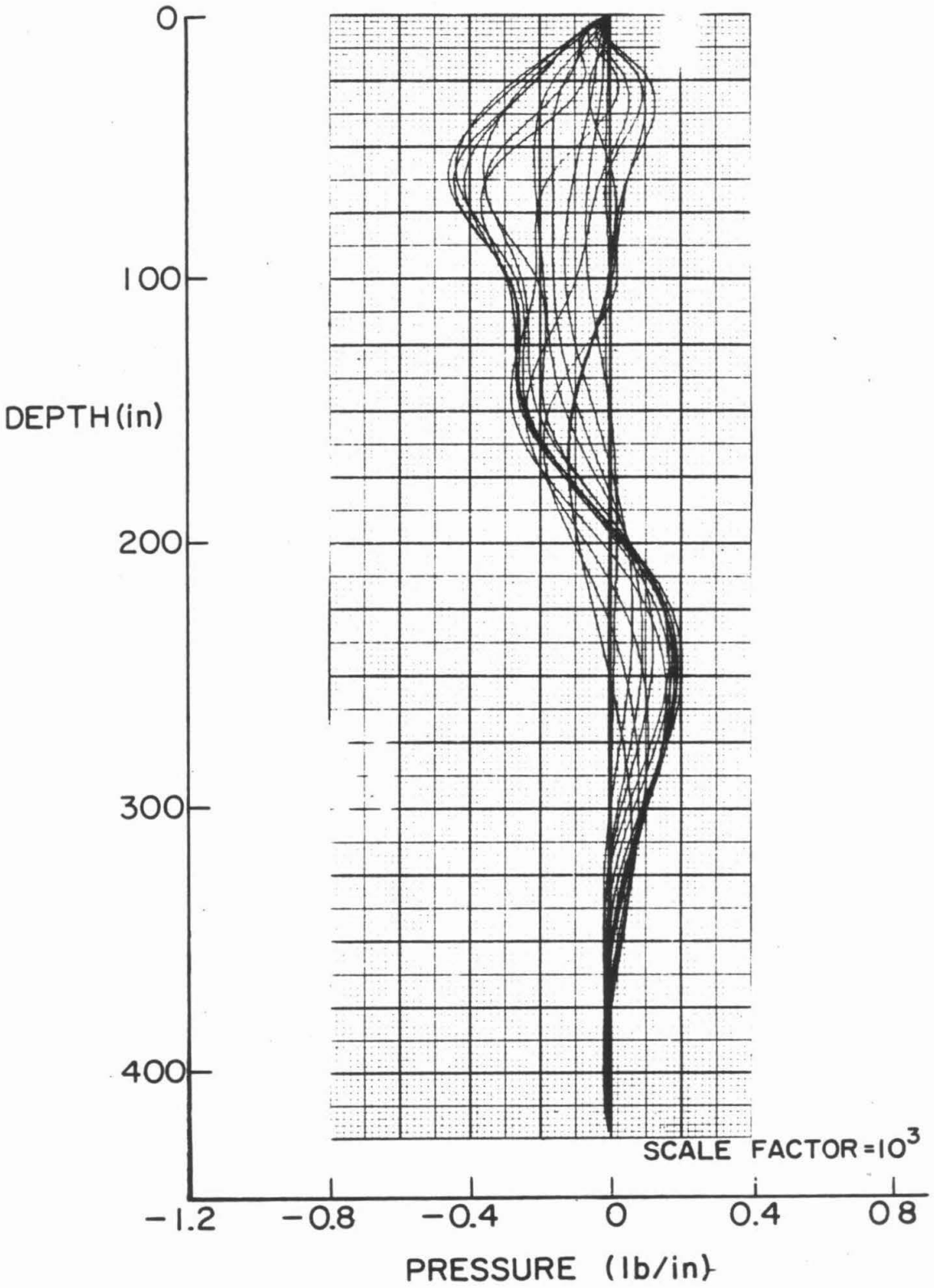

Fig. 7(b) Pressures.

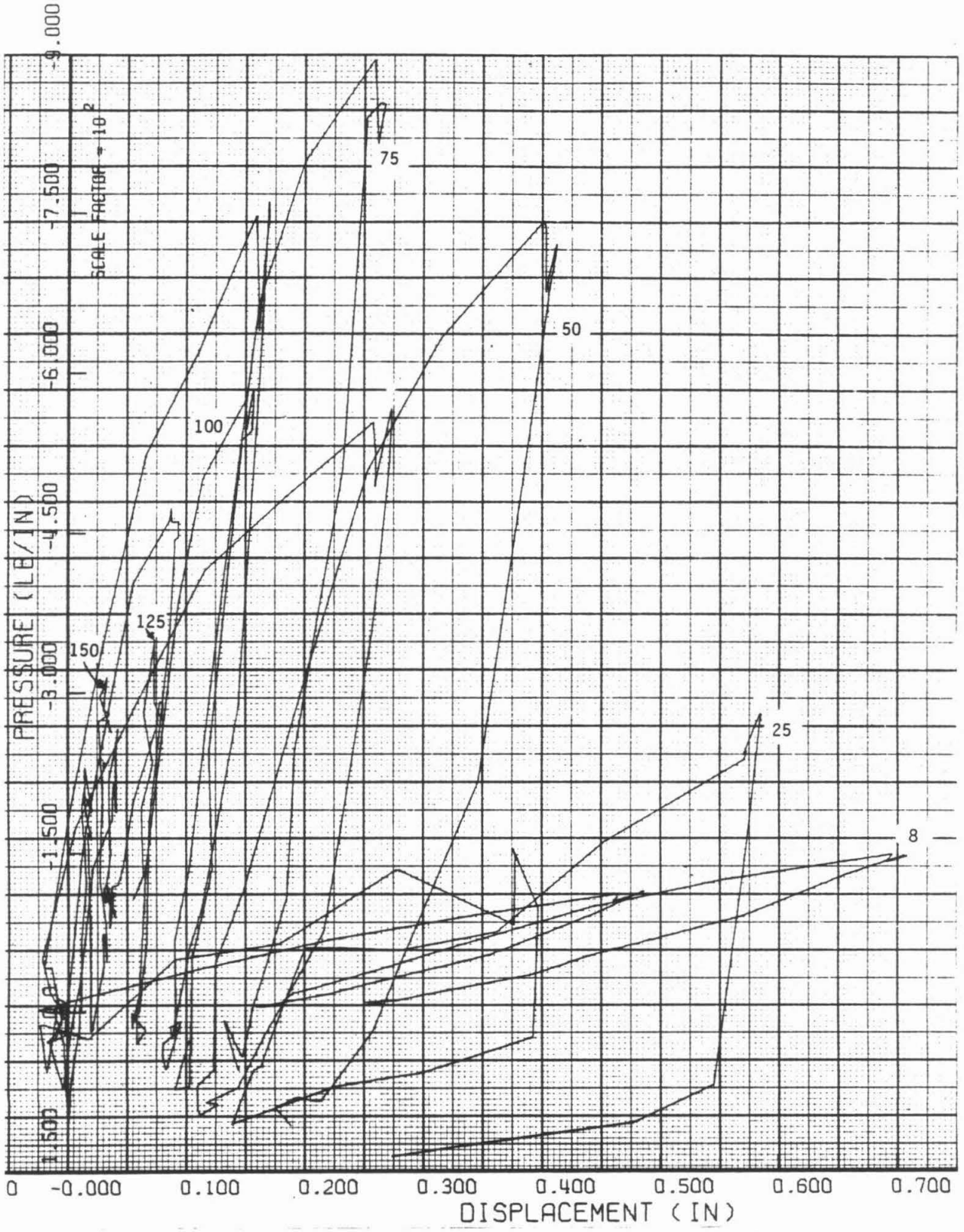

Fig. 8 Two loading cycles, dry soil, loading point at -0.5 inches soil interaction pressure versus displacement as a function of depth:

(a) All depths.

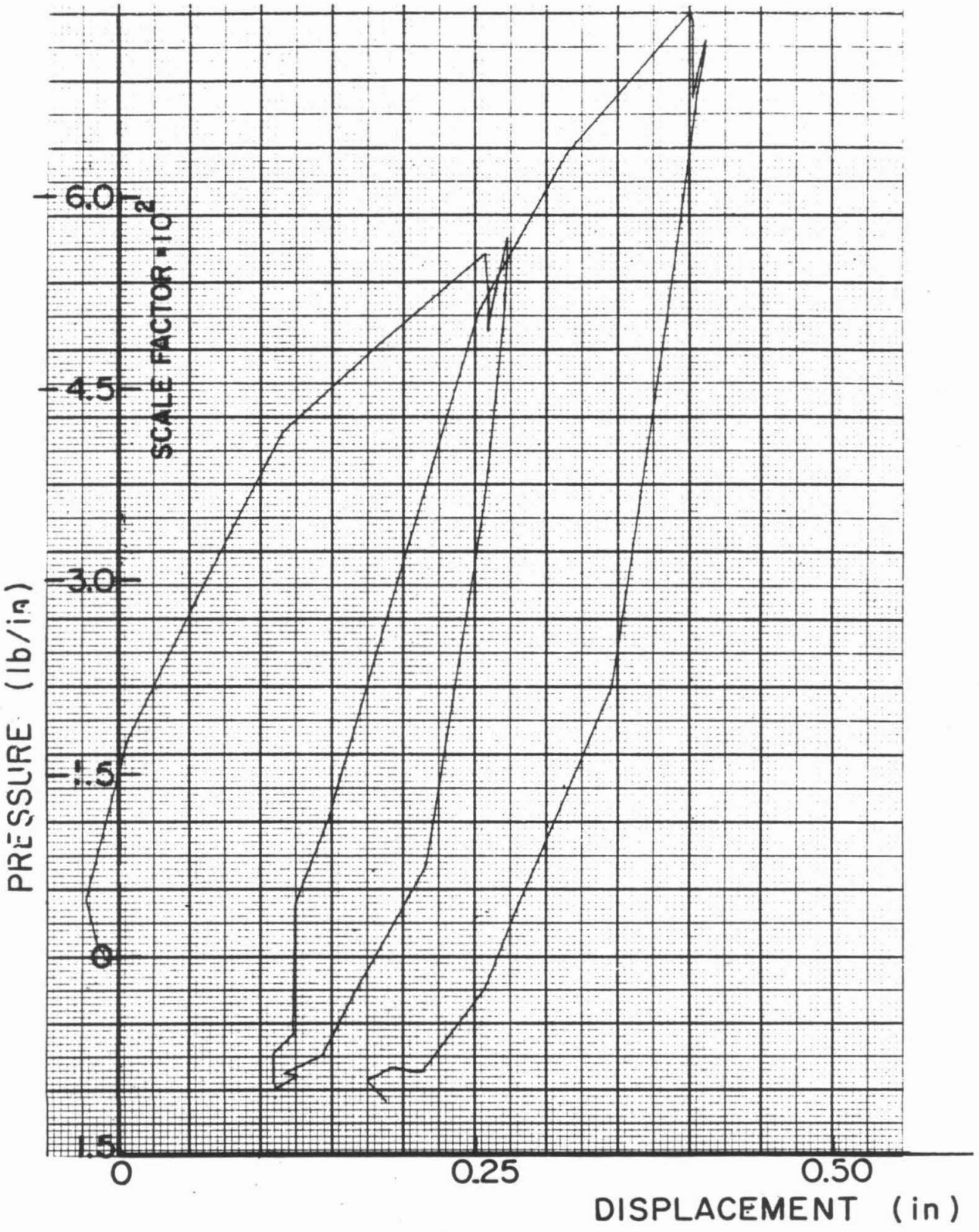

Fig. 8(b) 50 inch depth only.

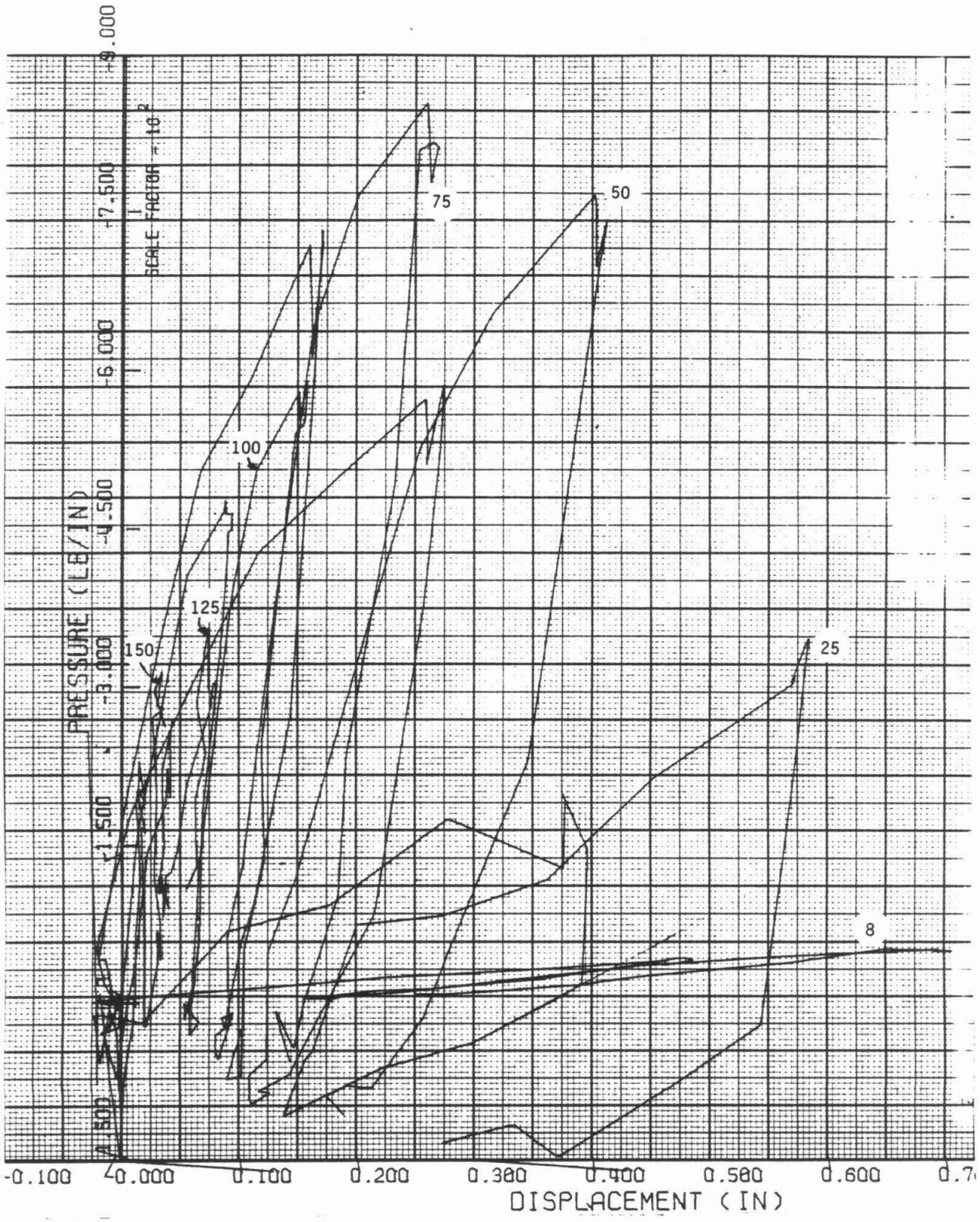

Fig. 9 Two loading cycles, dry soil, loading point at -0.2 inches, pressure versus displacement as a function of depth:

(a) All depths.

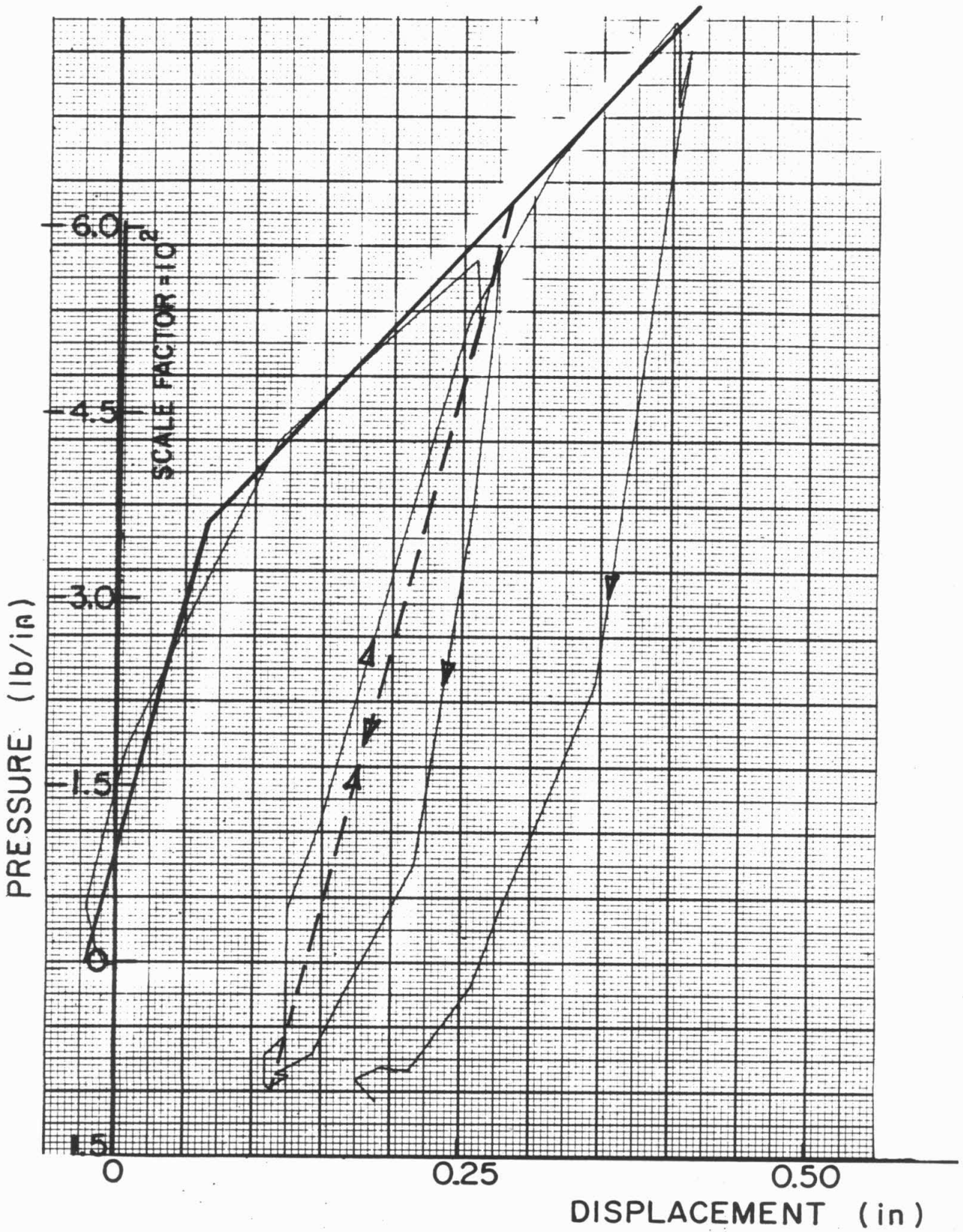

Fig. 9(b) 50 inch depth only.

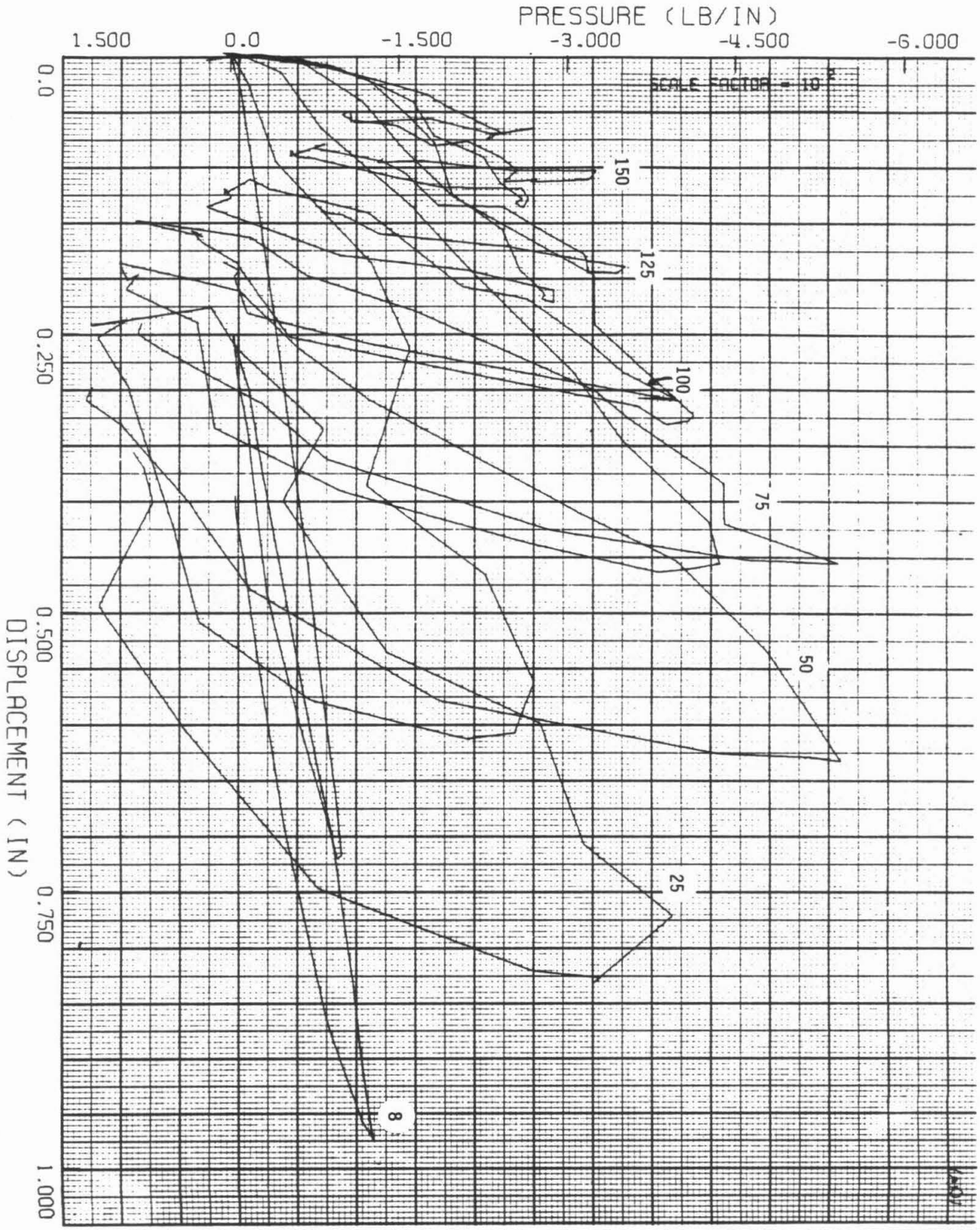

Fig. 10 Two loading cycles, saturated soil, loading point at -0.5 inches, pressure versus displacement as a function of depth:

(a) All depths.

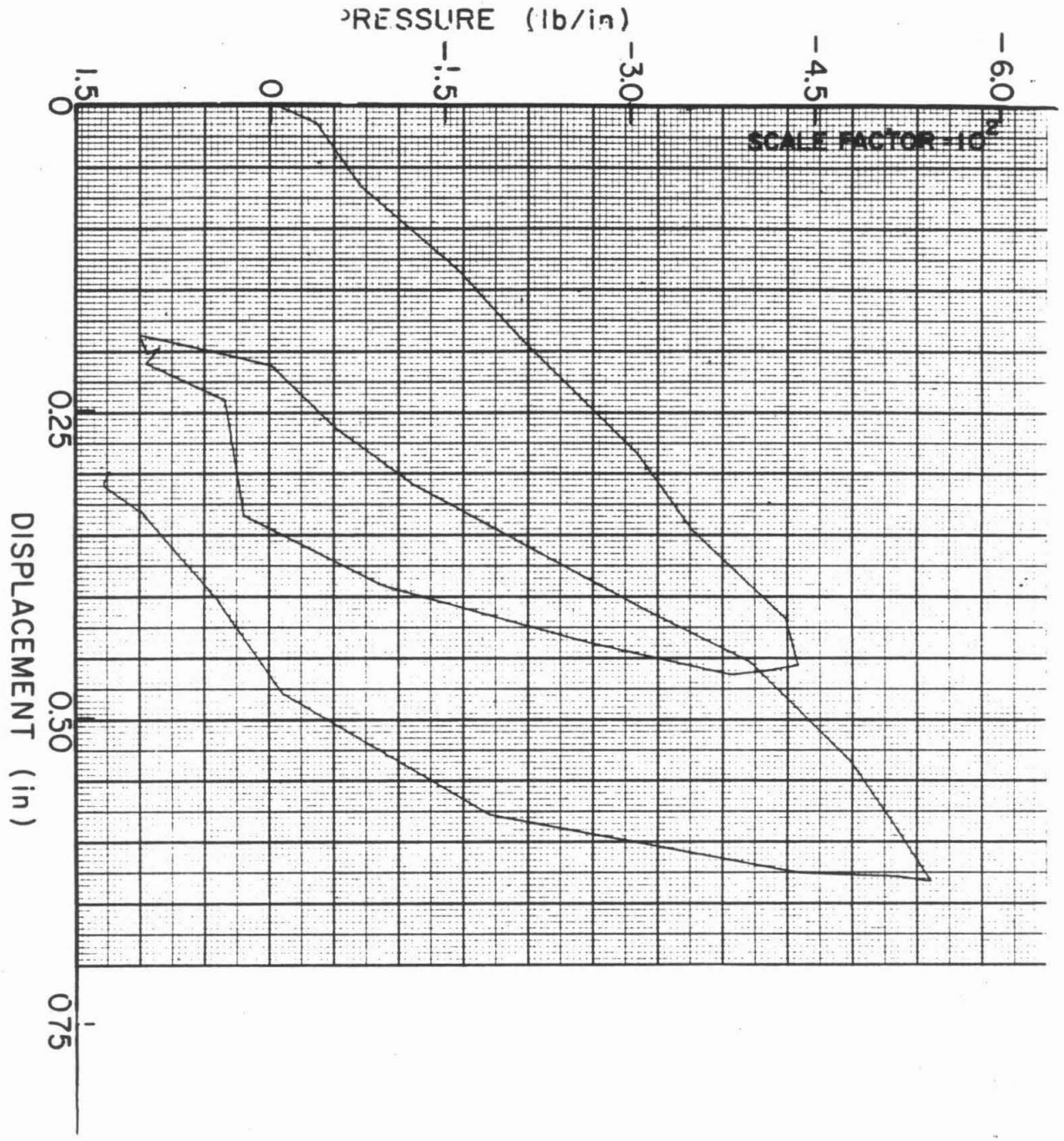

Fig. 10(b) 50 inch depth only.

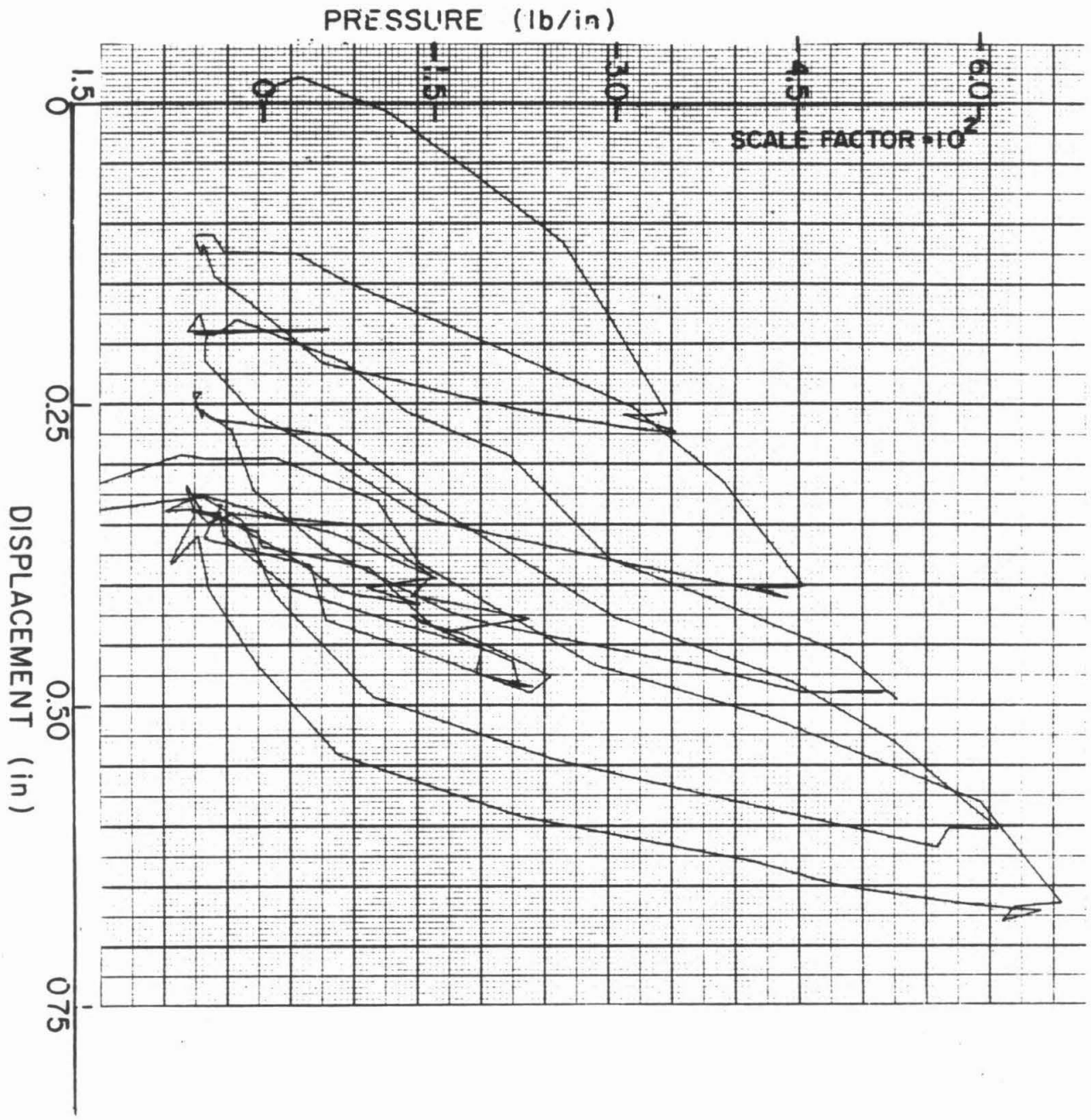

Fig. 11 Dry soil, loading point at -0.2 inches; pressure versus displacement at 50 inch depth for all 8 loading cycles.

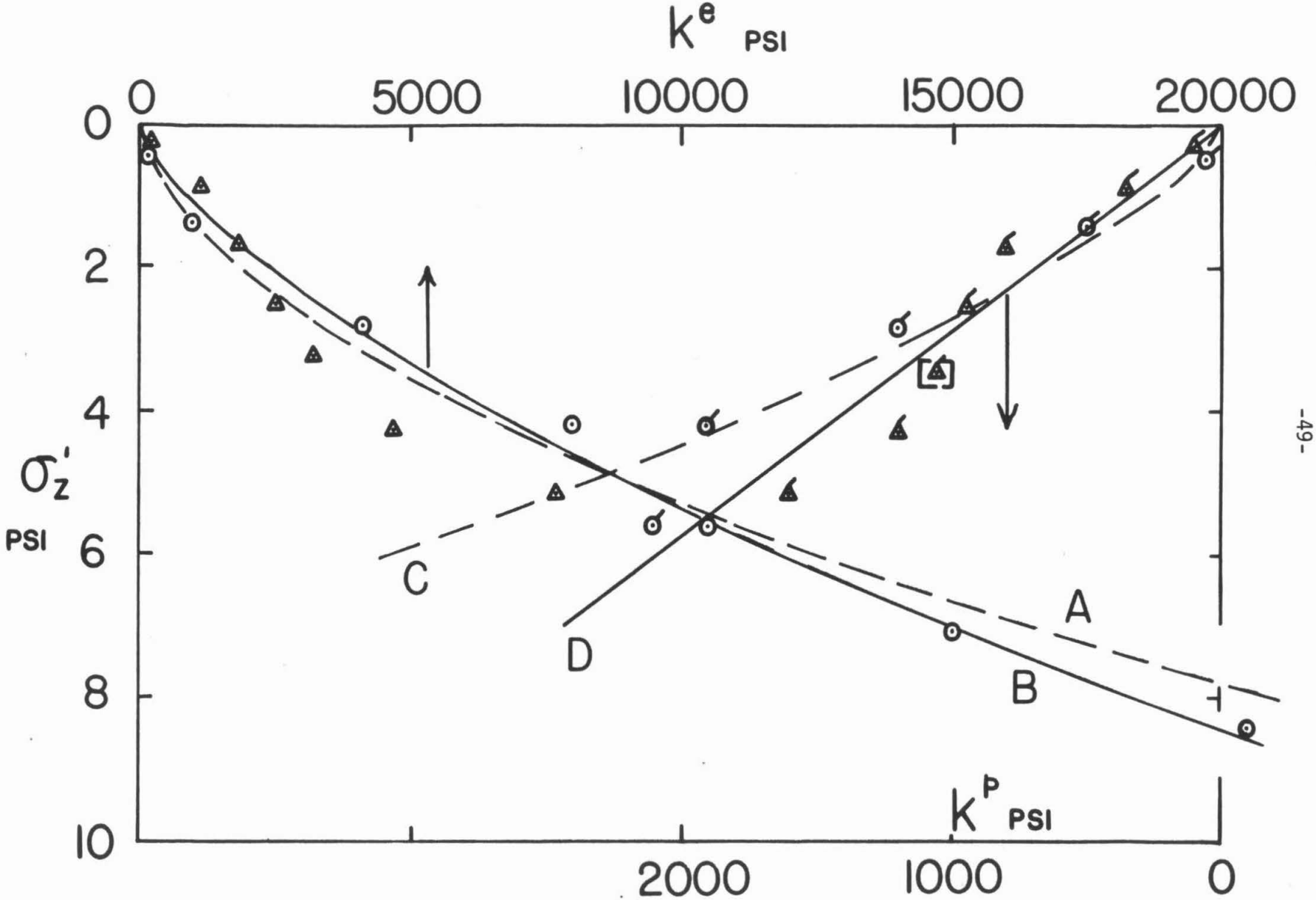

Fig. 12 Dry and saturated soils, elastic and plastic moduli versus vertical effective stress, and fitting curves: A - $k^e = 508(\sigma_z')^{1.792}$; B - $k^e = 818(\sigma_z')^{1.5}$; C - $k^p = 221(\sigma_z')^{1.466}$; D - $k^p = 350\sigma_z'$
Values in pounds per square inch (psi).

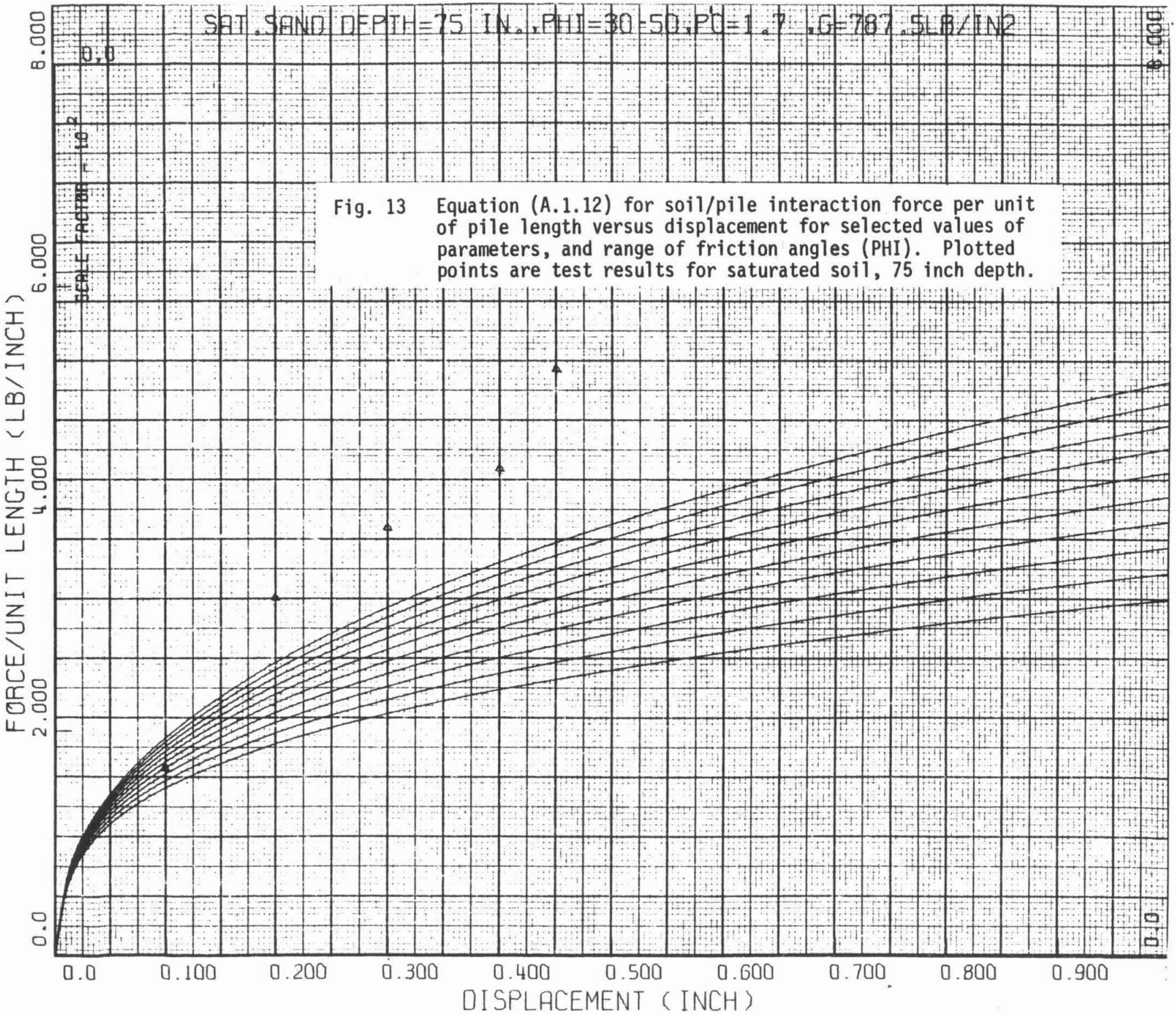

Fig. 13 Equation (A.1.12) for soil/pile interaction force per unit of pile length versus displacement for selected values of parameters, and range of friction angles (PHI). Plotted points are test results for saturated soil, 75 inch depth.

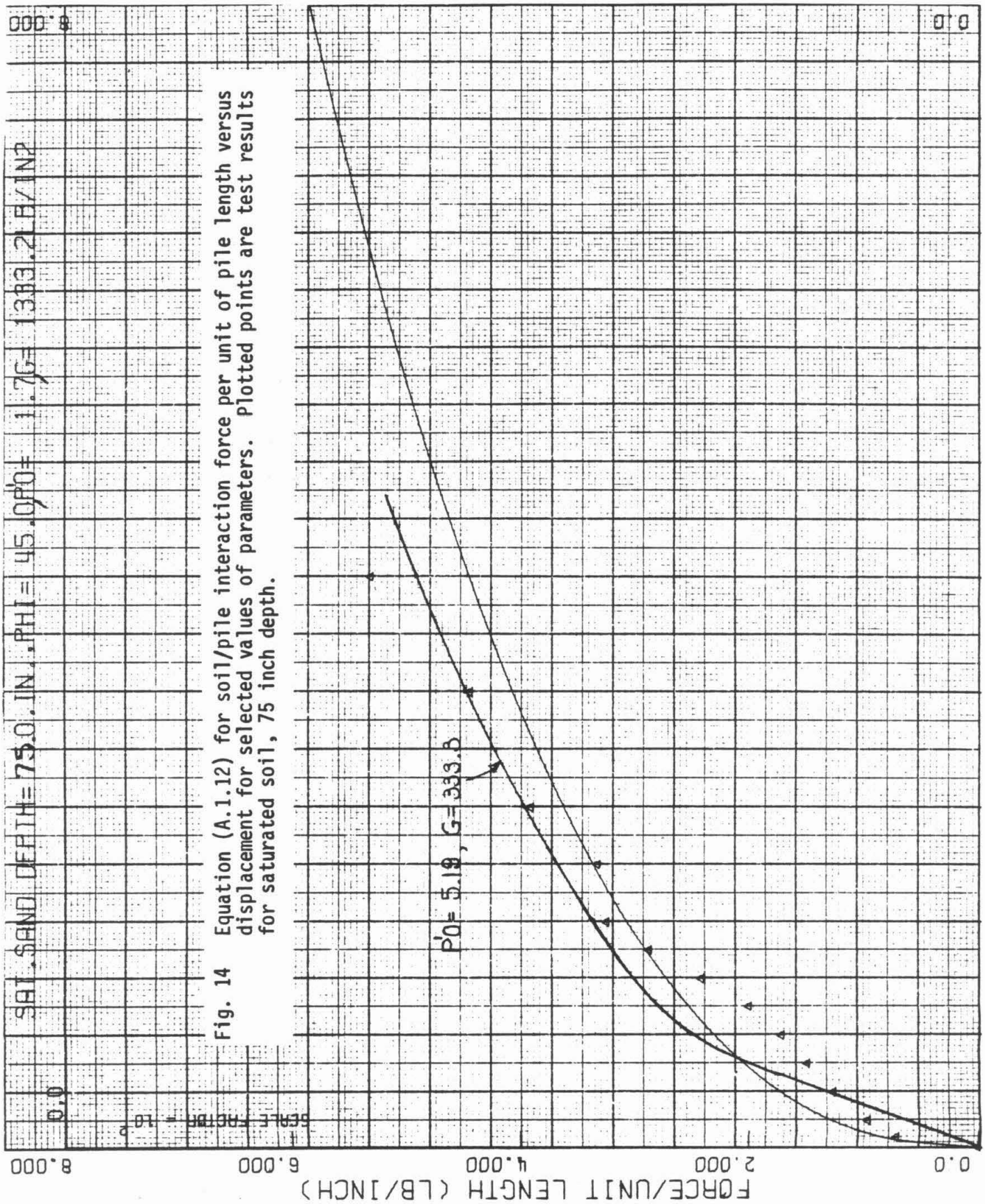

Fig. 14 Equation (A.1.12) for soil/pile interaction force per unit of pile length versus displacement for selected values of parameters. Plotted points are test results for saturated soil, 75 inch depth.

APPENDIX A

SOIL INTERACTION FORCE ON LATERALLY DEFLECTED PILE

The pile cross section is assumed to be cylindrical. After driving and before lateral load is applied, the pile is subjected to a lateral static effective pressure p_0', which may be greater than the at-rest soil pressure to an extent depending on the pile and the driving process (open- or closed-end pile, etc.). This effective pressure is shown in Figure A.1(a); the pore pressure is not shown since it will be assumed that lateral deflection of the pile in saturated sand will be slow enough that no pore pressures will be generated. In that case the resisting soil pressure to lateral displacement will be entirely due to effective stresses.

When the pile cross section of interest is displaced a distance u, the effective pressure becomes as shown in Figure A.1(b). This is a complicated distribution, which could be obtained only by a three-dimensional nonlinear or elastic-plastic analysis. The analysis has not been done, even on a linearly-elastic basis. Even if the pile cross section is assumed to deform the soil in plane strain as in the plane shown in Figure A.1, the linear analysis presents difficulties and has not been done. Consequently, an approximate plane strain elastic-plastic analysis is performed here, in order to see if it bears any resemblance to the results obtained from the centrifuge experiment.

The simplication is introduced of taking the problem as equivalent to expanding a cylindrical cavity to represent the pressure distribution at the front of the pile, and contracting a cylindrical cavity at the rear. Figure A.1(c) represents the two halves of this solution. It is assumed that

the soil will behave linearly elastically up to some lateral displacement, and thereafter exhibit plasticity. This approximation gives, of course, a pressure discontinuity at the sides of the pile, and ignores the friction there. However, the expansion assumption probably represents a soil pressure greater than the actual stress, and possibly the two effects will offset each other. It appears, at any event, as shown later, that the pressure at the rear of the pile contributes only negligibly to the force required to displace the pile, when the soil goes into the plastic range.

Clay soils will not be considered here, although a solution is available. For sand, the expanding plane strain cavity problem has been solved (for the pressuremeter) by Gibson and Anderson (3), whose solution has been verified in this study and is employed as follows:

1. Elastic Behavior

The pile radius is a_0, soil friction angle ϕ, shear modulus G, effective soil pressure on the front of the pile p_f', on the back, p_b', static lateral effective soil pressure p_0', and pile displacement u.

For the expanding cavity, it can be shown that the expansion is linearly elastic up to a soil pressure p_e' where

$$p_e' = (1 + \sin \phi)p_0' \qquad (A.1.1)$$

In the elastic lateral pressure range from p_0' to the value given by (A.1.1) the displacement is given by

$$u = \frac{(p' - p_0')a_0}{2G} \qquad (A.1.2)$$

Substituting for the limiting pressure p_e' from (A.1.1) in (A.1.2) yields the limiting elastic displacement

$$u_e = \frac{p_0' a_0}{2G} \sin \phi \qquad (A.1.3)$$

These results are obtained from Gibson and Anderson, who do not consider the contracting cavity. However, the corresponding results can easily be derived, to give the elastic range from the static lateral pressure p_0' <u>down</u> to a pressure p_c' where

$$p_c' = (1 - \sin \phi) p_0' \qquad (A.1.4)$$

The radial displacement in the elastic range is again given by (A.1.2), so that u is now negative, and substitution of the value of p_c' from (A.1.4) gives the limiting elastic displacement, u_c, in contraction,

$$u_c = - \frac{p_0' a_0}{2G} \sin \phi \qquad (A.1.5)$$

It is seen that the absolute values of u_e and u_c are conveniently identical so that as the pile moves laterally, its movement is linearly elastic both from the expansion and contraction points of view up to a displacement given by (A.1.3) and (A.1.5).

The behavior of the pile is now required in the elastic range. Equation (A.1.2) is used for response at both front and rear. Rearranging gives

$$p_f' = \frac{2uG}{a_0} + p_0' \qquad (A.1.6)$$

for the radial pressure on the front of the pile, and

$$p_b' = -\frac{2uG}{a_0} + p_0' \qquad (A.1.7)$$

for the pressure at the back. It is assumed that the reaction pressure on the pile, f, is given by equilibrium of the lateral forces acting on unit length of the pile (perpendicular to the paper; see Figure A.1.(c))

$$2a_0 p_f' - 2a_0 p_b' - 2a_0 f = 0$$

from which

$$f = p_f' - p_b' \qquad (A.1.8)$$

$$\text{or} \qquad f = \frac{4uG}{a_0} \qquad (A.1.9)$$

by substitution from (A.1.6) and (A.1.7). Now the net soil reaction force per unit length of the pile, F, is given by

$$F = 2a_0 f$$

so that

$$F = 8Gu \qquad (A.1.10)$$

As is also evident from a dimensional analysis of the problem, this reaction force is independent of the pile diameter. For a Winkler type of foundation analysis, the term 8G in (A.1.10) corresponds to the horizontal subgrade reaction coefficient k acting on the pile. Since G in sand varies with depth in some fashion, k will also vary with depth. The factor 8 in (A.1.10) comes from the geometry and assumptions involved in the analysis. A more exact analysis of a circular rigid inclusion moving laterally in a linearly elastic

medium in plane strain would give a result of the same form as (A.1.10) but with a numerical coefficient different from 8. The value 8 is probably too high.

2. Plastic Behavior

After the soil yields, an equation for the pressure required to expand the cavity has been given by Gibson and Anderson

$$p_f' = p_0'(1 + \sin\phi)\left\{\frac{2Gu}{a_0 p_0' \sin\phi}\right\}^{\frac{\sin\phi}{(1+\sin\phi)}} \qquad (A.1.11)$$

Although they did not treat the case of the contracting cavity, its equation can be obtained by replacing N by 1/N and u by -u in (A.1.11) as follows

$$p_b' = p_0'(1 - \sin\phi)\left\{\frac{2Gu}{a_0 p_0' \sin\phi}\right\}^{-\frac{\sin\phi}{(1-\sin\phi)}} \qquad (A.1.12)$$

Subtracting p_b' from p_f' as in (A.1.8) for f, in the plastic domain gives, eventually

$$f = p_f'\left\{1 - \frac{1 - \sin\phi}{1 + \sin\phi}\left[\frac{2Gu}{a_0 p_0' \sin\phi}\right]^{-\frac{2\sin\phi}{\cos^2\phi}}\right\} \qquad (A.1.13)$$

in which the second term in the brackets represents the pressure contribution from the back of the pile. In general, it is very small and can be ignored. Thus the force per unit length of the pile in the plastic range is given approximately by

$$F = 2a_0 f = 2a_0 p_f' = 2a_0 p_0' (1 + \sin\phi)\left[\frac{2Gu}{a_0 p_0' \sin\phi}\right]^{\frac{\sin\phi}{(1+\sin\phi)}} \qquad (A.1.12)$$

A plot of log F versus log u tends towards a straight line of slope $\sin \phi/(1 + \sin \phi)$; thus a plot of experimental results could be used to determine the friction angle of the soil, if the present model is valid. Unfortunately, the slope is not very sensitive to ϕ. For soils, ϕ lies in the range 30° to 45° for which the slope ranges from 0.333 to 0.414. Scatter in the computer-processed data can easily obscure the slope of a line at this level of discrimination. When the dry sand data from depths of 25, 50 and 75 inches were plotted on a log-log graph, they indicated fairly high friction angles of around 45° but the model is sufficiently questionable that this, although plausible, cannot be taken as a reliable value.

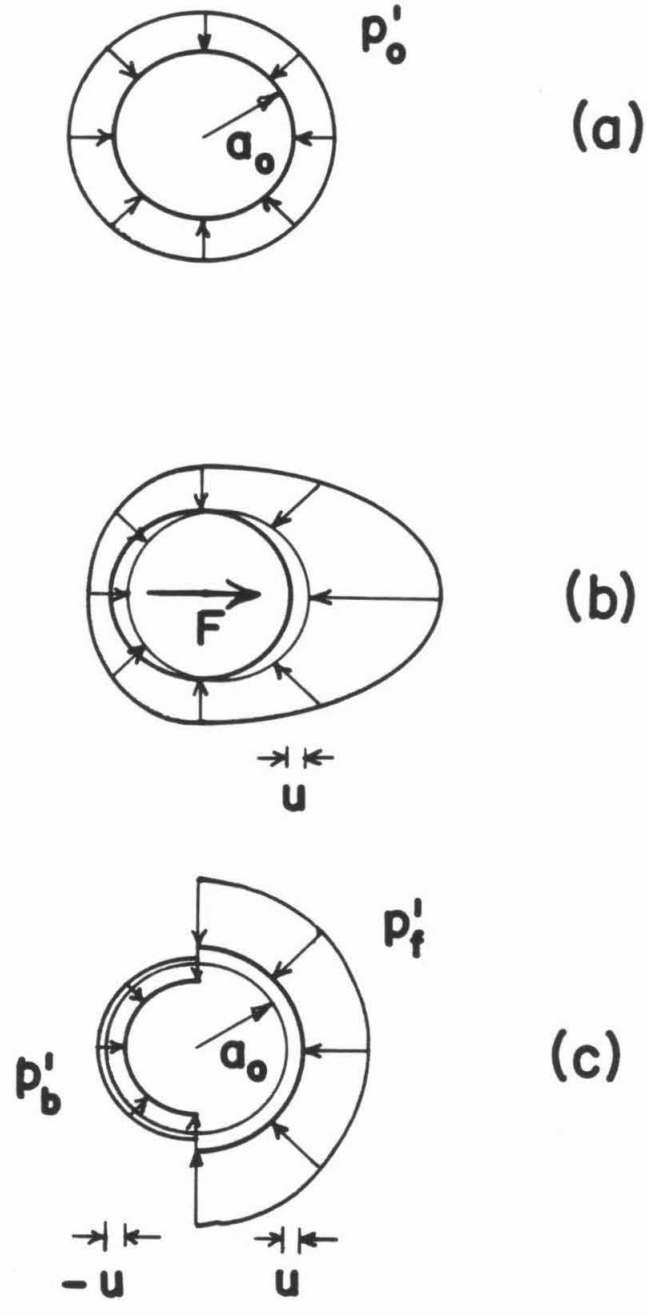

Fig. A.1 Approximate analysis for lateral pile displacement in plane strain: (a) Static effective stress on pile; (b) Effective pressure redistribution when pile displaced distance u; (c) Approximation when right side of pile expands radius by u, left side contracts radius by -u.